CHALMERS

Optimization of Bending Wave Loudspeakers

Master's Thesis in the Master's programme in Sound and Vibration

RODRIGO MARTÍNEZ REDONDO

Department of Civil and Environmental Engineering
Division of Applied Acoustics
Chalmers Room Acoustics Group
CHALMERS UNIVERSITY OF TECHNOLOGY
Göteborg, Sweden 2007

Optimization of Bending Wave Loudspeakers

Master's Thesis in the Master's programme in Sound and Vibration

RODRIGO MARTÍNEZ REDONDO

Optimization of Bending Wave Loudspeakers
Master's Thesis in the Master's programme in Sound and Vibration
RODRIGO MARTÍNEZ REDONDO

Optimization of Bending Wave Loudspeakers
Master's Thesis in the Master's programme in Sound and Vibration
RODRIGO MARTÍNEZ REDONDO
Department of Civil and Environmental Engineering
Chalmers Room Acoustics Group
Chalmers University of Technology

Abstract

The Distributed Mode and Bending Waves Loudspeakers are recent developments that have provoked much interest over the past few years. The papers published on the subject have highlighted the differences between these classes of loudspeakers comparing them to a conventional pistonic radiator.

In this project, a flat Bending Wave Panel Loudspeaker (BWL) was built. The aim of this project is to combine a BWL with a passive projection screen. Employing Hamada's "Stereo Dipole" we should be able to create very convincing virtual images around a single listener for Virtual Reality applications.

First, an introduction into this technology will be presented where some theoretical concepts will be explained to provide in-depth understanding.

Secondly, all the measurements that have been carried out to optimize the behaviour of the panel, regarding different structures and excitation methods will be presented showing the best solution found. Damping mechanism will allow us to simulate the desired infinite behaviour, which will facilitate the "Stereo Dipole" technique. Finally, we will introduce the final configuration of the panel.

Keywords: Bending Waves, Critical Frequency, Virtual Source Imaging, Damping, Piezoelectric sensor, NXT technology, Manger transducers, Mechanical Impedance.

II

Acknowledgements

First of all, I would like to thank Dr. Mendel Kleiner, for giving me the opportunity to work in the field I like, for being such a nice supervisor, and especially for the interest and confidence he showed.

I would like to acknowledge Börje Wijk, Pontus Larsson and Gunilla Skog for all the help with the administrative and technical matters. I will not bother you anymore with annoying harware or software problems.

I want to thank Anders Genell for giving us his exciters so kindly, and specially for showing me where I could find good old vinils.

A big thanks to the master and exchange students at Applied Acoustics of the year 2007 for being really good friends and such a fun group. I can not mention each of you individually, but you know who you are. I hope our paths will cross again somewhere else.

I would like to thank all my Spanish friends of Göteborg, for making this experience even better. See you all this summer.

Finally, I would like to thank my family for all the support, visits and good Spanish meat they sent me.

IV

Contents

Chapter One

Introduction

The permanently ongoing search for new kind of acoustic transducers which can improve the radiation characteristics and response for audio applications lead the researchers to the bending wave radiation. The excitation of bending waves on plates or panels results in significant sound radiation with valuable qualities such as a diffuse sound field and a wide directivity which is largely independent of frequency. Therefore, vibrating panel loudspeakers find their development in more and more areas, such as displays, car audio and communication devices.

These kinds of structures can be supported by a flat panel or plate, with very low mass and rigidity. The aim of this work is to build a flat Bending Wave panel using the Hamada's "Stereo Dipole" which can create virtual images around a single listener, and it can also act as a passive screen where images can be projected, simulating then a virtual reality environment for binaural applications. It will be optimized in terms of critical frequency and sound radiation features.

The theory involved in the vibrational behaviour of flat structures and the associated important theoretical facts that will be investigated empirically such as critical frequency, point impedance or damping, as well as it sound radiation characteristics will be presented at Chapter 2.

Chapter 3 will show some model simulations that have been carried out in order to find out the most important parameters that might influence sound radiation and critical frequency. The exciter technology has been modeled as well to see the influence of the moving-coil system into the whole structure.

Section 4 is focused on the measurements that allowed us to decide which was the best solution in terms of optimization. Several material and thicknesses were tested, as well as three different excitation methods, to see the influence in the behavior of the panel. The Transfer Function for each alternative is included.

The last chapter introduces the final configuration. The "Stereo Dipole" technique will be explained in detail, as well as the features of the line configuration. The damping concept that was introduced at chapter 2 is now tested in the real structure, to see its performance and characteristics. Finally, the structure will be presented and its transfer function measured.

The last part will draw some conclusion of the work. Further procedures that could not be done in the time of the work will be introduced as well.

Chapter Two

Bending waves theoretical behavior

2.1 Introduction

In contrast to sound in gas fluids, which only allow one type of wave, i.e. longitudinal wave, there is a large variety of structure borne sound waves. The most important group regarding sound radiation, which we are dealing in this work, are bending waves, also called flexural waves.

First of all, they are mainly responsible for the radiation of sound from vibrating plate-like structures. The reason for this can be explained in the displacement of the elements in the wave. This displacement component appears in the normal direction to the surface of the structure.

In Figure 2.1 the vibration pattern of bending waves is shown. As we can see, it combines both longitudinal and transversal motion. As we see, the cross sections are moving perpendicularly to the equilibrium line, rotating around the normal axis.

Compression

Expansion
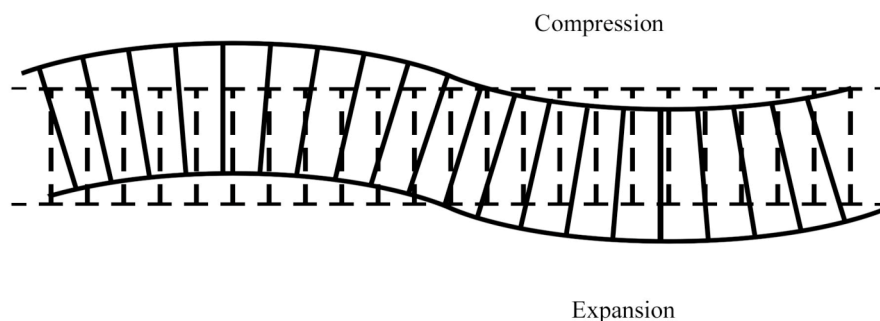
Figure 2.1   Illustration of bending waves in a beam. The bending wave amplitudes have been highly exaggerated.

It is also important to note that bending waves are waves that appear in thin media, since one or two of the cross-sectional dimensions are smaller than the governing wavelength for plates and beams, pure longitudinal waves cease to exist in these structures.

This chapter is focused on give a wide knowledge of the theory involving bending waves, in order to be able to control them with sound radiation purposes. First, the main features will be presented, giving special attention to the general laws and equations which govern infinite one dimensional propagation on beams, called the Euler-Bernoulli theory. Secondly, the same will be show for two dimensional media on plates, using the Kirchoff's theory.

We will see that the velocity of the wave is different at each frequency in the same medium. This phenomenon is called *dispersion*.

The final part is focused mainly on bending wave sound radiation and its quantities. *Critical frequency* will be introduced, as well as the concept of *damping*, useful when we deal with infinite plates such as bending wave loudspeakers.

2.2 One and two-dimensional Bending Waves

Bending waves are associated with comparably large transverse vibration amplitudes leading to a significant disturbance of the adjacent fluid, and therefore, a change also in the sound radiation. The good coupling between bending structures and fluids indicates that the impedance of the transversal motion and the sound waves in the fluid are of similar magnitude [1].

On the contrary to the other structure-borne sound waves, bending waves are represented by four field variables instead of two: the transversal velocity v_y, the angular speed ω_z, the bending moment M_z, and the force F_y. To make it clearer, the four field variables and their positions are illustrated on a single beam element.
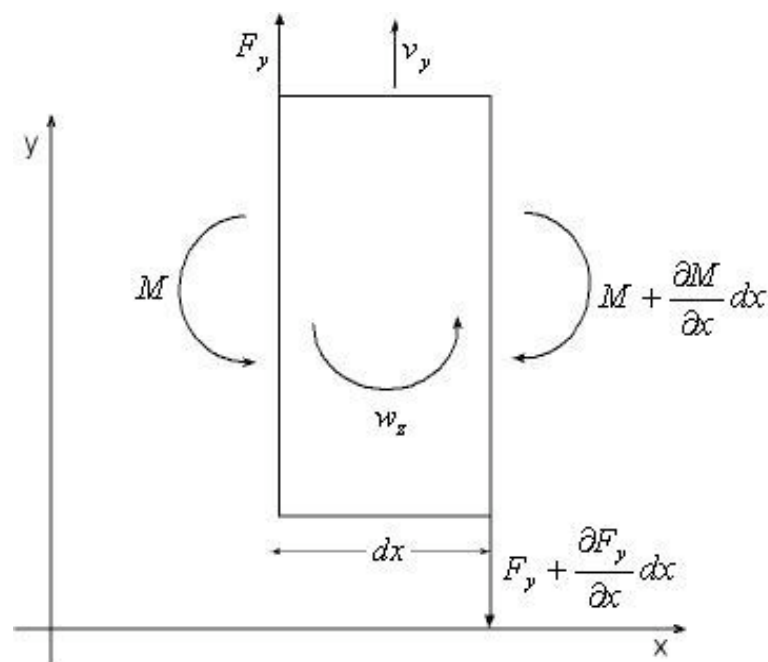
Figure 2.2   Indication of the field variables and their directions of bending waves.

Between these four variables there are four differential relations cyclically related, which are used to find the wave equation that governs the motion. Moreover, the boundary conditions become more difficult when we work with this type of waves. A wider description can be found at [2].

In the following two subsections the wave equation is presented for one-dimensional case on beams and two dimensional cases on plates. Both theories contain simplifications, which are mainly the assumption of a non-deformed cross section (i.e. infinite high shear stiffness) and the cancellation of rotational inertia. When the bending wavelength becomes comparable with the thickness of the plate or beam, these two facts lead to erroneous results. Therefore, it yields an upper frequency limit. To compensate this, extended theories, i.e. Timoshenko or Mindlin theories are developed which hold further up in frequency. However, in most cases the simple Euler-Bernoulli theory is sufficient and therefore preferable for the scope of this work.

2.3 Bending Wave's Equations

2.3.1 One dimensional case (Euler-Bernoulli theory for beams)

A beam is shown in Figure 2.3 where bending waves are propagating. We consider beams with thickness and height much smaller than its length and also than the associated wavelength.

$$\frac{\partial \beta}{\partial x} dx = \frac{\partial' \eta}{\partial x} dx$$

$$\beta + \frac{\partial \beta}{\partial x} dx$$

$$\eta + \frac{\partial \eta}{\partial x} dx$$

$$\beta \qquad \eta$$

$$\beta = \frac{\partial \eta}{\partial x}$$
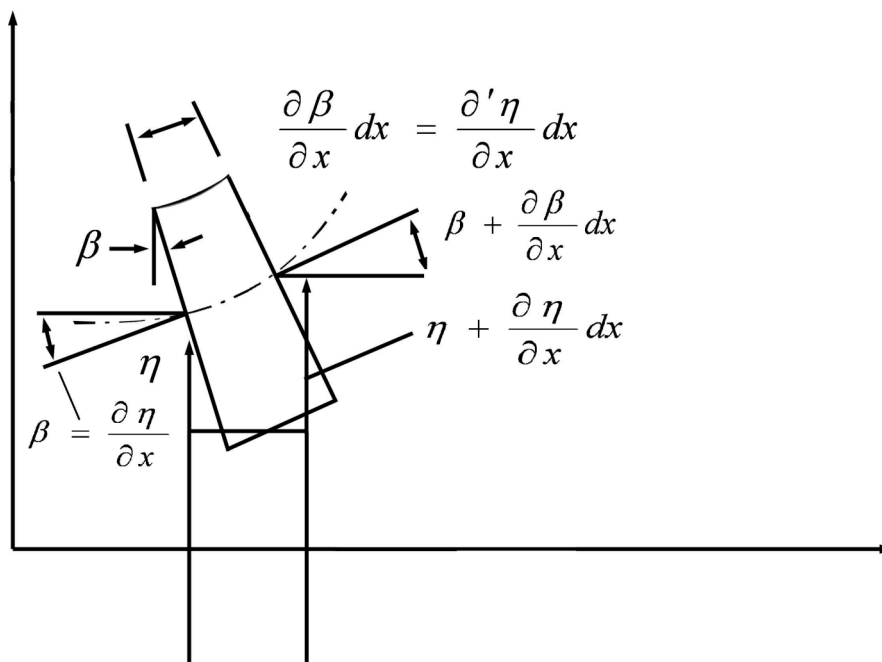
Figure 2.3   Variables and deformation of a beam element in bending motion.

Analysing the figure, one can conclude that the bending wave angle   is related to the displacement in the normal direction   by the equation:

$$\beta = \frac{\partial \eta}{\partial x}. \tag{2.1}$$

Differentiation with respect to time the leads:

$$\omega_z = \frac{\partial v_y}{\partial x}. \tag{2.2}$$

As shown in [3], the rate of change of the angular velocity with distance is given by:

$$\frac{\partial \omega_z}{\partial x} = \frac{\partial^2 v_y}{\partial x^2} = \frac{\partial}{\partial t}\left(\frac{\partial^2 \eta}{\partial x^2}\right). \tag{2.3}$$

The bending angle will cause a certain bending moment M_z which depends on the bending stiffness of the material B and the change of the bending angle over x:

$$M_z = -B\frac{\partial \beta}{\partial x} = -B\frac{\partial^2 \eta}{\partial x^2}. \tag{2.4}$$

Where B is known to be the bending stiffness, which is the product of the modulus of elasticity (which is a material property) and of the moment of inertia (which is a characteristic of the cross-section):

$$B = EI. \qquad \text{Being} \qquad I = \frac{1}{12}bh^3. \tag{2.5}$$

The expression which relates the shear force F_y to the bending moment M_z may also be obtained from static bending theory [2]:

$$F_z = -\frac{\partial M_z}{\partial x} = \frac{\partial}{\partial x}\left(B\frac{\partial^2 \eta}{\partial x^2}\right). \tag{2.6}$$

Now, applying Newton's second law of motion, over a force changing over x:

$$\frac{-\partial F}{\partial x} = m'\frac{\partial^2 \eta}{\partial t^2}. \tag{2.7}$$

Where m' the mass per unit length of the bar,

$$m' = \rho w h.$$

Where   is the density, w the width and h the height of the beam. Substituting the force in Eq.2.6 one finally obtains the wave equation for bending waves in one dimension and assuming that the bending stiffness is constant (which is correct in most of the cases) the equation can be simplified to:

$$B \frac{\partial^4 \eta}{\partial x^4} = -m' \frac{\partial^2 \eta}{\partial t^2} \,. \tag{2.8}$$

This wave equation differs substantially from the longitudinal and transversal wave equations due to a fourth derivative in space instead of the usual second derivative. However, the resulting solution will have the form of a simple harmonic wave:

$$\eta(x,t) = \eta_A e^{-jkx} e^{jwt} \,. \tag{2.9}$$

If one substitutes this equation into (2.8) then one finds that this expression satisfies the differential equation, as long as the radial frequency and the wave number obey:

$$\frac{B}{m'} k_b{}^4 = \omega^2 \,. \tag{2.10}$$

We can see clearly that the wave number on a beam is frequency dependant, following:

$$k_b(\omega) = \sqrt[4]{\frac{\omega^2 m}{B}} \,. \tag{2.11}$$

Knowing that $k = \dfrac{w}{v}$, it will lead to:

$$v(\omega) = \sqrt[4]{\frac{B}{m'}} \sqrt{\omega} \,. \tag{2.12}$$

On the contrary of velocity of sound of air, when we are dealing with beams or plates, the velocity is frequency dependant. This important effect is called dispersion, where we will be discussing it in another section.

Taking into account the boundary conditions, the complete solution of the bending wave equation can be found in some literature, such as [1].

$$\eta(x,t) = \left(\eta_+ e^{-jkx} + \eta_- e^{jkx} + \eta_{+j} e^{-kx} + \eta_{-j} e^{kx} \right) e^{jwt} \tag{2.13}$$

The four exponential terms represent four different waves. The first two are waves propagating in the positive and negative x-directions. The other two solutions are so-called bending near fields, which are deformations of the beam decaying exponentially with the distance to the excitation point and oscillating with the excitation frequency. These near fields can be caused by an excitation but also by the presence of boundary conditions.

2.3.2 Two dimensional case (Kirchoff theory for plates)

The Kirchoff theory for bending waves in plates is based on the same simplifications as the Euler-Bernoulli theory, that is, assumptions of infinite shear stiffness and negligible rotational inertia. The wave equation is:

$$B_x \frac{\partial^4 \eta}{\partial x^4} + 2B_{xz} \frac{\partial^2 \eta}{\partial x^2} \frac{\partial^2 \eta}{\partial z^2} + B_z \frac{\partial^4 \eta}{\partial z^4} + m'' \frac{\partial^2 \eta}{\partial t^2} = 0. \tag{2.14}$$

B_x and B_z are the bending stiffness in the x-and-z directions. B_{xz} is a mixed term. For isotropic plates, B_x and B_z are identical whilst for orthotropic plates they can differ. Isotropic plates will be considered throughout the whole of this investigation. Therefore, B' is defined as the two-dimensional bending stiffness per unit length:

$$B' = \frac{EI'}{1 - \mu^2}, \tag{2.15}$$

Where   is the Poisson constant and I is the cross section moment of inertia per unit length for a plate of thickness h. The bending stiffness of the plate differs from that of a beam due to the constraint in the z-direction.

$$I' = \frac{1}{12} h^3. \tag{2.16}$$

We can draw an analogy for the resolution of the one dimensional case in Sec.2.3.1, finding:

$$\eta(x, z, t) = \eta_A e^{-j(k_x x + k_z z)} e^{jwt} \tag{2.17}$$

The bending wave number k_b can be written as:

$$k_b^2 = k_x^2 + k_z^2 \tag{2.18}$$

Inserting Eq. 2.17 into the general solution 2.14 will lead to:

$$B' k_b^4 = m'' \omega^2. \tag{2.19}$$

In this case, the velocity is also frequency dependant which will be discussed later. Note here we use B' and m'' instead B and m'. Like in the one dimensional case, the Kirchhoff theory also requires a fourth partial differential equation of difficult resolution, with more complicated boundary conditions. This is the reason for using another method to calculate the modal density and behaviour of a plate, such as Finite Element Analysis. The modal density has to be sufficiently large to produce a superposition of modes with different amplitudes, producing a continuous spectrum.

2.4 Bending Wave's Behaviour

2.4.1 Dispersion

As we discussed in the previous sections, both one-dimensional and two-dimensional bending wave numbers are frequency dependent. Is easy to infer in Equation 2.11 that it is dependant on the square root of the angular frequency, unlike the usual linear frequency dependence in air, according to $k = \omega/c$.

This fact leads to a "phase velocity" on bending waves which is also frequency dependant, according to Equation 2.12.

For plates of thickness h, it may be simplified to:

$$c_b = c_{mat}\sqrt{\frac{1.8h}{\lambda_{mat}}}$$

(2.20)
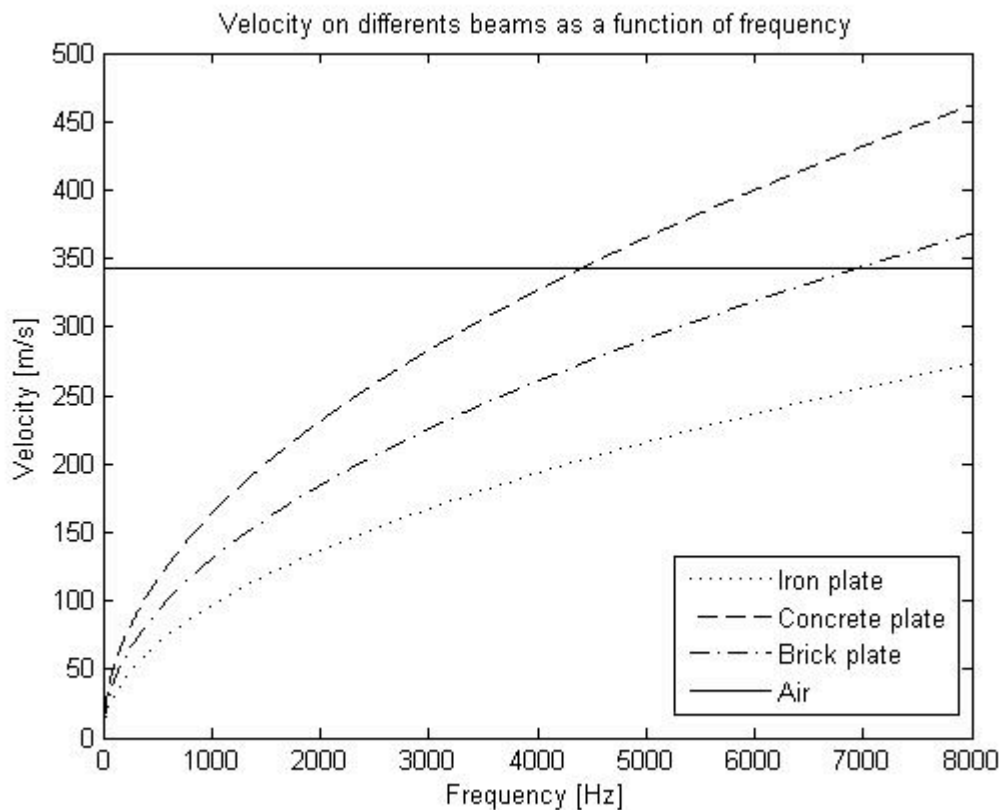
Figure 2.4   Bending wave velocity on plates made with different material, with the reference of the velocity on air. Data for the iron plate: c_{iron}=517 m/s, h=10mm; Concrete: c = 370 m/s, h = 4cm; Brick: c=235m/s, h = 4 cm.

As we can see in figure 2.4, there is no upper limit for the phase speed of bending waves, which violates physics. The reasons for this failure are the

certain simplifications that were introduced when deriving the bending wave equation; at high frequencies, the bending waves are transformed into transversal waves, which are non dispersive, and therefore has a constant velocity above the transition point. The limit of applicability of the analytical representation is defined in [2] as:

$$\lambda = 6h$$

There is a 10% error in equation 2.20, when the wavelength is on the order of six times the thickness of the beam.

Another interesting effect of dispersion is the distortion of the signals travelling in dispersive medium. For a non-dispersive medium, all frequencies travel with the same speed. Since the phase speed in this case is frequency dependent, higher frequencies will propagate faster than lower frequencies and the form of the signal will therefore be distorted. This effect can clearly be seen in the figure below.
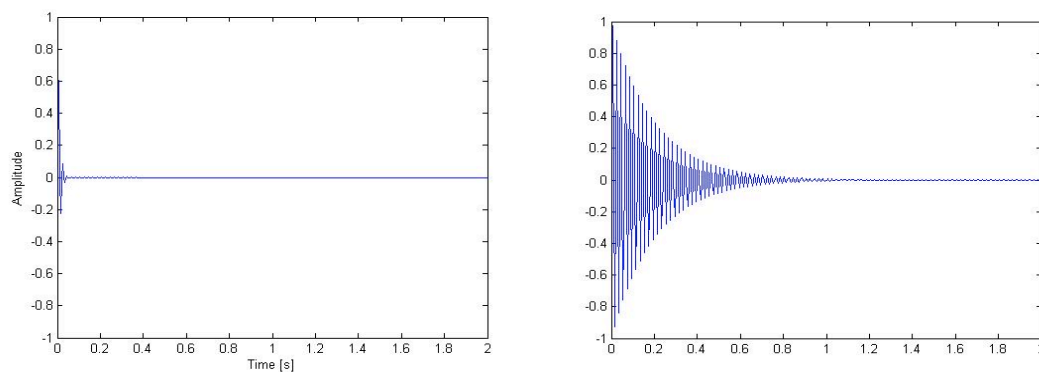
Figure 2.5   Pulse distortion due to dispersion effect of a beam.

2.4.2 Driving point impedance of Homogeneous Plates

One of the most important concepts when we work with waves is the Impedance Z, which relates the force over the velocity in a specific area.

Specification of the excitation region when we are dealing with impedances is needed to define it. It is clearly easier for the case where the exciting force acts only at one point. – Or in practical terms, on a region whose dimensions are considerably smaller than the wavelength of interest. In this case, the impedance is determined at the excitation point, and it is called "Driving point impedance".

The most straightforward method for deriving the driving-point impedance of a plate consists of solving the differential equation 2.14. A complete guideline is given in [2], being finally found that:

$$Z_0 = \frac{\hat{F}_0}{\hat{\underline{v}}_0} = \frac{8B'k^2}{\omega} = 8\sqrt{B'm''} \qquad\qquad (2.21)$$

This simple result, which has been well validated by experimental measurements in [4] is rather surprising. The input impedance of a plate seems to be real, and frequency independent. Thus, could be considered in an electric analogy like a resistor with a value given by 2.21.

It can be useful in further sections to find an expression for the velocity distribution on a plate [2], being:

$$\hat{\underline{v}}(x,z) = \frac{\hat{F}_0\omega}{8B'k^2}\left[H_0^{(2)}(kr) - H_0^{(2)}(-jkr)\right] = \frac{\hat{F}_0}{Z_0}\left[H_0^{(2)}(kr) - H_0^{(2)}(-jkr)\right] \qquad (2.23)$$

Where $H_0^{(2)}$ is the Hankel function of the second kind. For further simplifications, one may use the asymptotic expressions for the Hankel function, instead of a more exact representation.

$$H_0^{(2)}(x) \approx \frac{2j}{\pi}\ln x \qquad\qquad \text{for} \quad |x| << 1 \qquad\qquad (2.24)$$

$$H_0^{(2)}(x) \approx \sqrt{\frac{2}{\pi x}}e^{-j(x-\pi/4)} \qquad\qquad \text{for} \quad |x| >> 1 \qquad\qquad (2.25)$$

2.4.3 Critical frequency

As already pointed out in section 2.4.1, the dispersive behaviour of bending waves play a significant role in the fluid-structure interaction.

Looking at figure 2.4, we can easily infer that there is a point where the bending wave velocity is equal to that of sound waves in the surrounding fluid at the so-called critical frequency, f_c. The critical frequency is sometimes also called the coincidence frequency. Using the condition $c_B=c$ one finds the expression for the critical frequency as:

$$f_c = \frac{c^2}{2\pi}\sqrt{\frac{m''}{B'}} = \frac{c^2}{1.8c_l h} \qquad\qquad (2.26)$$

Where c is the sound velocity of the surrounding medium, c_l the longitudinal wave velocity in the plate material and h is the plate thickness.

For any material we deal with, this is only possible for one single frequency for which $_B =$, since the bending wavelength increases following:

$$\lambda_B = 2\pi \sqrt[4]{\frac{B'}{\omega^2 m''}} \, ,\qquad\qquad (2.27)$$

While the wavelength of air increases inversely with the angular frequency:

$$\lambda = \frac{2\pi c}{\omega} \qquad\qquad (2.28)$$

One may note from eq.2.26 that the critical frequency only depends on the stiffness of the plate and the mass per length, and hereby increasing the mass or decreasing plate stiffness we can get higher critical frequency, and the other way around to decrease f_c.

As it is outlined in [2], there are some important insights concerning the strength and direction of sound radiation from bending waves. One can divide the frequency range into two different regions:

Bending waves that are longer than the wavelength in the ambient medium, $\lambda_B >$, or in other words, bending waves having a frequency above f_c (fast waves) causes a directionality effect, which is associated with relatively strong radiation.

On the other hand, for $\lambda_B <$, where waves are propagated at smaller velocities, (slow waves), the hydrodynamic short-circuit effect results in a considerable reduction of radiation, and consequently, efficiency is also reduced. Nevertheless, this working range is chosen instead to achieve a diffuse sound field of low directivity.

Therefore, the critical frequency is one of the most important parameter related to sound radiation, which can easily be determined just by the ratio of mass and bending stiffness.

2.4.4 Modal Vibration of Bending Waves

When dealing with finite structures, the requirement for the existence of standing wave patterns is already fulfilled, due to the termination of the structure.

In the boundaries, the travelling wave and the reflections can interfere. At certain frequencies, all waves travelling on the beam will be in phase, generating a pure standing wave pattern which is called modal pattern or natural mode. Each modal pattern has natural frequency associated to it, which defines the frequencies at the structure would cause vibrating after an excitation. In contrast to infinite structures which can vibrate freely *at any frequency*, finite systems can only vibrate freely at *its natural frequencies*.

A finite structure which is exposed to a continuous signal will vibrate at the excitation frequencies, but the spatial distribution will consists of a superposition of many modes with different amplitudes.

In a sound radiation point of view, if the infinite structure is not excited at a natural frequency, the response of the structure will consist of a superposition of many modes.

Therefore, vibrating patterns involving only a few modes can also result in less sound radiation than each individual mode would produce.

Furthermore, when many modes are excited, the interference pattern will again lead to an interruption of the cancellation since the modes will be decorrelated some degrees. Hence, it is desired to excite as many modes as possible by the source. Therefore, it is of importance to have a high modal density in the frequency range of operation.

The bending wave modal density however turns out to be constant, irrespective of frequency because of the frequency dependent phase velocity of the bending waves.

At high frequencies, the average number of modes for bending waves in a sheet having a surface area of S in a frequency band of width f is:

$$\Delta N \approx \frac{S}{2}\sqrt{\frac{m''}{B'}}\Delta f$$

Typically at least 10 modes have to be present in the frequency range of interest.

But since the human perception of frequency is logarithmic, a constant modal density in reality leads to a lack of modes per frequency band at low frequencies.

To avoid this effect, several measurements could be done. The positions of the excitation points can be chosen in a way to excite as many modes as possible, that it is, the positions have to be placed where no node line of a mode is present.

This is the working principle of Distributed Mode Loudspeakers, which will be presented in the next chapter.

2.4.5 Bending wave's attenuation

As we can infer with the content of the previous sections, there are two different parameters, related with structural properties of the plate, which strongly determine the sound radiation and the available frequency range: mass and stiffness. In this section, we will introduce the concept of damping, which has capital importance when we want to simulate infinite plates, as in the scope of the work.

With damping mechanism we mean all mechanism which transform vibration energy, which implies some kinetic and some potential energy, into a different form of energy, for instance, heat. This energy is then losses in the vibrating system.

There are different methods to describe damping processes. The main difference between these models is their frequency dependency, which leads to different values of the complex modulus. Normally, we can expect a quite constant loss factor, therefore, the lost factor model is chosen, which is defined in [3] as:

$$\eta = \frac{E_{loss}}{2\pi E_{rev}}. \tag{2.29}$$

Where E_{loss} is the lost energy per period and E_{rev} the reversible energy.

There are several ways to damp a material, divided in two main categories: Non material damping mechanism and material damping mechanism. In this work, we will follow the procedure on [5], since we use the damping material to simulate an infinite plate, which can be achieved cancelling the reflections at the edges. Therefore, an attached layer of damping material will lead to absorb the waves at the boundaries. Usually, the lost energy of the single plate can be neglected. Then, an expression for E_{loss} and E_{rev} for the attached layer is given in [3]:

$$E_{loss} = \pi \eta_2 E_2 d_2 \left| \frac{\partial \xi_m}{\partial x} \right|^2 . \tag{2.30}$$

Where h_2 is the thickness of the material, E_2 its Young's modulus, and d_2 its loss factor. $_m$ is the displacement of the neural axis line of the attached layer, which can be expressed by the bending angle and the distance a between the neural axis of the coupled system and the middle line of the attached layer.

$$\xi_m = a\beta \tag{2.31}$$
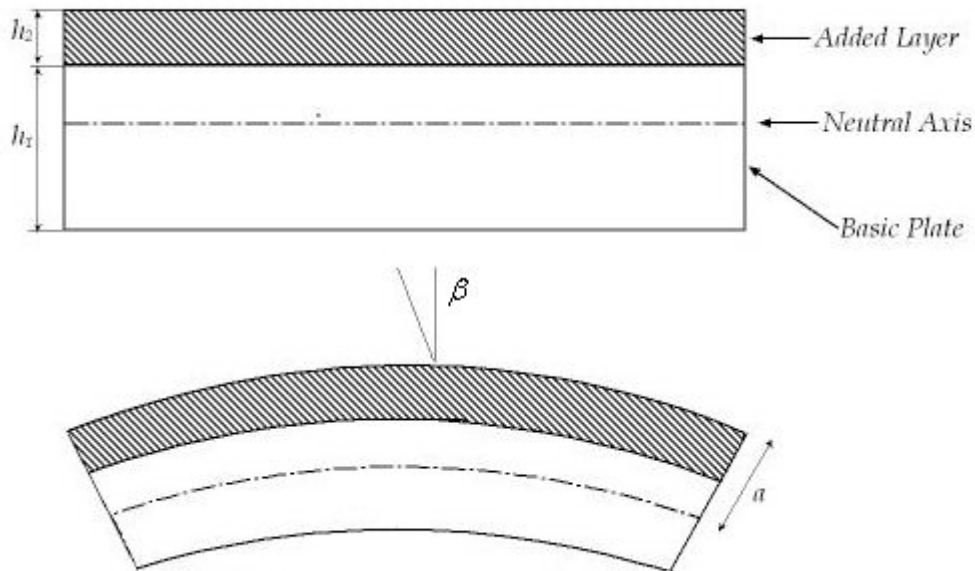
Figure 2.6   Deformation of a beam with viscoelastic layer.

The reversible energy is given by the potential energy stored in the bending of the whole structure.

$$E_{rev} = \frac{1}{2} B \left| \frac{\partial \beta}{\partial x} \right|^2 .$$

(2.32)

With the equations 2.31 and 2.32 we can express the loss factor of the complete structure for bending waves:

$$\eta_b = \eta_2 \frac{E_2 h_2 a^2}{B} .$$

(2.33)

The expression above still contains two quantities which have to be determined: *a* and *B*. Only if the stiffness of the attached layer is small in comparison with the stiffness of the plate the neural axis will still equal the middle line of the plate. Then the distance:

$$a = \frac{h_1 + h_2}{2}$$

(2.34)

The derivation of the bending stiffness is more complicated, but it is shown in [3] that yields:

$$B \approx \frac{E_1 h_1^3}{12} + E_2 h_2 a^2$$

(2.35)

As a conclusion, it is therefore important that the elastic layer is as thick as possible (the total damping increases with increasing thickness h_2), and the damping layer therefore should have a high loss factor h_2 present in equation 2.33. It should have high modulus of elasticity as well. Useful damping materials generally consist of filled high-polymer plastics, with modulus of elasticity greater than 10^{10} dyn/cm^2 and with as high loss factor as possible.

2.5 Bending Wave's Sound Radiation

2.5.1 Introduction

For comparison and optimization purposes of the built loudspeaker structure, a deep understanding of the airborne sound radiation is required. The sound radiation behaviour depends to a great extent of the characteristics of the loudspeaker. So the geometric forms, material properties and kind of excitation are of great importance to determine the sound radiation of the plate.

In this section, the basic mechanisms of the air-interaction will be discussed for infinite structures, which are what we are dealing for. Since the medium

where the radiation will interact is air, we can disregard the radiation loading and damping quantities. Moreover, the sound radiation below the critical frequency yields to diffuse behaviour, the radiation directivity will not be mentioned deeply since it is out of the scope of the work.

The discussion of radiation and general remarks for simple configurations such as spherical point sources, monopole and dipole sources, can be found at [3]. This method describes the sound pressure of the vibrating plate summing up the contributions of all equal monopoles. The disadvantage of this method is that one has to know the velocity of the plate very well. Due to the difficulties to determine that value, can be useful so to describe the radiation in another terms, especially for a quasi-infinite plate excited for both point source and line source.

An infinite structure excited by a point source create free bending waves on the far field, but it also entail a flexural near field close to the source. The radiation of this near field constitutes almost all the sound power radiation when we are at sub-critical frequencies, where we are dealing for. For that reason, it is strongly important to find an expression for that sound radiation.

2.5.2 Point excitation

In this sub-section, an expression to determine the sound power level of plate excited by a point source will be developed. Again, radiation loading is disregarded.

The sound power radiated by the point source can be written after further simplifications as:

$$P = \frac{\rho_0 c \omega^2 |F_0|^2}{4\pi B'^2} \int_0^k \frac{k_0 k_r dk_r}{\left[k_r^4 - k_B^4\right]\sqrt{k_0^2 - k_r^2}}. \qquad (2.36)$$

For $k \ll k_B$, that is, for bending wavelengths that are smaller than the wavelength in the ambient medium, into another words, below the critical frequency, one can rewrite:

$$P = \frac{\rho_0 c \omega^2 |F_0|^2}{4\pi B'^2 k_B^8} \int_0^k \frac{k_0 k_r dk_r}{\sqrt{k_0^2 - k_r^2}} = \frac{\rho_0 c k^2 |F_0|^2}{4\pi \omega^2 m''^2} = \frac{\rho_0 |F_0|^2}{4\pi c m''^2} \quad \text{for} \quad f \ll f_c \qquad (2.37)$$

That means that for sub-critical frequencies, the radiation of sound power of point-excited infinite plates is independent of frequency. The flat frequency response that can be achieved is evidently the most important feature on loudspeaker design. Furthermore, we just need the input force and the mass per unit area to calculate it. This independence of stiffness is due because an increase in stiffness leads to longer wavelengths, and thereby to an increase in sound radiation, but it also results in a decrease of the excitation.

One can realize this fact easily rewriting the equation 2.37 using the driving point impedance (Eq. 2.21):

$$P = \frac{16\rho_0 c k^2 B'}{\pi\omega^2 m''^2}\hat{v}_0^2 = \frac{16\rho_0 c k^2}{\pi k_B^4}\hat{v}_0^2. \tag{2.38}$$

Expressing the ratio B'/m'' in terms of the critical frequency, it will lead to the following relation:

$$P = \frac{16\rho_0 c^3 \hat{v}_0^2}{\pi\omega_c^2} = \frac{4}{\pi^3}\rho_0 c^3 \hat{v}_0^2 \lambda_c^2. \tag{2.39}$$

With $\lambda_c = c/f_c$ the critical wavelength. Thus, the radiated power decreases as the plate stiffness decreases, and with higher critical frequency.

One can compare this value with the radiation of a baffled piston moving with the same velocity as the plate, driving a homogeneous plate. This comparison shows that the flexural near field radiates as much sound as the mentioned baffled piston with radius $\lambda_B\sqrt{2/\pi^3}$, which is roughly a quarter wavelength.

This theoretically constant radiated power for sub-critical frequency is not achieved empirically. We are dealing with a quasi-infinite structure, which is not entire real. When the acoustic wavelength becomes of the order of the characteristic dimensions of the panel, an interaction between the front and backside occurs. For that reason, at very low frequencies, the radiation characteristics of the structure changes to a dipole behaviour, with and associate lower efficiency.

One may use this simple result to estimate the radiation when the source in not a point source anymore, but rather a circle with radius a. The flexural nearfield will act like a piston with radius= $a + \lambda_B/4$ resulting in a radiated power:

$$P = \frac{\rho_0 c}{4}k^2 \hat{v}_0^2 \pi (a + \frac{\lambda_B^2}{4})^4. \tag{2.40}$$

In practice it is usually much more convenient to use the sound power level, instead of absolute units. This level is defined as:

$$L_P = 10\log\frac{P}{P_{ref}}dB. \tag{2.41}$$

Where $P_{ref} = 10^{-12}$ watts.

Finally, the following equation allows us to get the desired sound pressure level at a distance R from the source, assuming uniform propagation in all directions:

$$L_p = L_P - 10\log\left[\frac{2\pi R}{m^2}\right]dB \tag{2.42}$$

Where $2\pi R$ is the surface area of the hemisphere where the sound passes though at a distance R from the source.

2.5.3 Line excitation

As we will see in the next section, a line excitation may be a good choice in terms of Sound power radiated for the bending plate. For that reason, in terms of optimization of the present structure, the line excitation might be of interest. Therefore, brief understanding of its basic principles and equations is required. The complete derivation can be found at [7].

A plate drives with a line-shape excitation of force F_l with length l, which is large enough compared to the wavelength of the sound in the air can be expressed in terms of Sound power by the following equation:

$$P_l = F_l l \frac{\rho_0}{\omega_c m''} \tag{2.43}$$

Where F_l is the force per unit length l. As is easy to infer, an increase on the frequency will lead to a decrease in sound power. As in the foregoing section, we may rewrite the equation 2.43 in terms of velocity:

$$P = \frac{4}{\pi^3} v_0^2 l \rho_0 c \lambda_c^3 \tag{2.44}$$

Again, comparing the sound power emitted for the near field of a "quasi-infinite" structure with the one obtained when we are dealing with a baffled piston with the same particle velocity as the excitation line, one can found that the plate can radiate as much sound power as a piston of area $S = 4\lambda^3 l / \pi^3$. Here again, we must assume a frequency range below the critical frequency f_c.

2.5.4 Radiation ratios

One generally desires to know not only the radiated power, but also the relation between the structural vibrations and that power. This relation is usually described in terms of the so-called radiation efficiency, defined as:

$$\sigma = \frac{P}{\rho_0 c S \widetilde{v}^2} . \tag{2.45}$$

To find the value of this radiation efficiency one must know the average root-mean-square velocity of the radiating surface. When we are dealing with highly damped structures as in the purpose of this work, it is really difficult to

measure the velocity, because that velocity can vary considerably from point to point. Thus, one may not be able to define a meaningful average velocity or the corresponding radiation efficiency.

As defined in [6], a more meaningful radiation ratio in the scope of this thesis could be the radiated power of the optimized structure under treatment related with the original structure before the optimization treatment:

$$SPL_{inc} = 10\log\left(\frac{P_{opt}}{P_{prev}}\right) \qquad (2.46)$$

Now, it is possible to define and analyze the results of the optimization easily.

Chapter Three

Simulation Models

3.1 Introduction

The foregoing section have established the basic principles and behavior of bending waves, their sound radiation and damping processes. Focusing the purpose of this work, a model based on the previous work [5] is presented, in order to find the critical features and constants that define the sound radiation when we are dealing with this kind of loudspeakers. The following section will treat with the selection of the plate material, in order to improve its sound radiation.

After this selection, some MATLAB calculations will be presented to see the influence of the material parameters in its efficiency and working range.

3.2 Bending Waves Loudspeakers parameters

3.2.1 Working principles

The Distributed Mode and Bending Wave Loudspeakers is a recent development that has provoked much interest over the past few years [8-10]. These papers published on the subject have highlighted the differences of this class of loudspeaker to a conventional pistonic radiator.

In general, we can subdivide the loudspeakers which work with the bending wave principle in two principal groups:

DM Loudspeakers concerns a flat, thin, and light panel that radiates acoustics energy efficiently by exciting bending wave modes, and designed in such a way to obtain optimal modal distribution and where the driving point is also selected for optimal modal coupling. Therefore, reflections at the boundaries are produced and they will lead to pure standing wave patterns. The radiation produced is considered spatially diffuse, and it tends to a smooth function of frequency, combined with a pretty constant directivity.

In contrast, Bending Waves Loudspeakers are sufficiently damped at the edges so that the bending wave reflections as well as the radiation from the edges are neglible. This idea was developed by Manger Sound Transducer [A]. Josef W. Manger relied on the principle of bending waves, which starting from the centre of a plate-like diaphragm, travel to the outside. The rigidity of this thin flexible panel increases from the centre to the outside at an equal ratio, very similarly to the basilar membrane in our ear. High frequencies quickly run out in the inner area of the membrane, whereas long waves (low frequencies) concentrically reach right to the edge at the star-shaped damper. There they are absorbed so that no reflections can come from the edge.

Therefore, it behaves as an infinite surface, as it was stated in the previous chapter.

The previous structure was designed following the manger transducer principle, that it is, to build a pseudo-infinite plate, due to the easier way to control sound radiation in that way. Therefore, we will follow the same procedure.

3.2.2 Parameters

Bending wave loudspeakers can be made from a number of materials enabling a range of both acoustic and mechanical properties to be realised. By carefully selecting materials one can control the main parameters such as:

- Surface density.
- Bending Stiffness.
- Location of the Drive point.
- Damping and its function with frequency.

As we stated before on subsection 2.4.3, the critical frequency is the most important parameter, since we want to avoid strong directional radiation, which occurs above the critical frequency. Hence, we want to drive the plate below that frequency, which can be easily determined from a simple static measurement of the ratio of the mass per area unit to the bending stiffness, following Eq.2.26. For the purposes of the loudspeaker, it might be sufficient to achieve a critical frequency around 16 kHz.

This parameter is directly proportional to the Young Modulus and the thickness h. Therefore, a low rigidity of the material may yields to a higher critical frequency. But, in addition, to that, the rigidity is important in terms of visualization: Using a very elastic material will lead to unwanted vibration of the plate and it may also influence the visualization and the image might become bleary. Moreover, the unwanted vibration will disturb the intentional vibration of the exciters.

In terms of sound radiation, and according to Eq.2.37, the mass per unit area takes a capital role in the near-flexural field radiation. The less mass the higher SPL can be achieved. This mass is function of the thickness and the material density. Thus, a light and very thin material has to be used.

Concerning the loss factor, which must be necessary high, in order to absorb the reflections at the boundaries; it affects the bending stiffness according to Eq.2.35. Nevertheless, it is not taken into account into this modelling. The localization of the driving point is not really important, since we are dealing with an infinite plate, and no modal node will be matched.

3.2.3 Sound Power level calculations

Some calculations regarding Sound Power level have been made with different materials, to see the influence of the parameters mentioned above.

There are several ways to characterise a source. The most common and representative way is the Sound Pressure Level as a function of frequency. As we can see at Eq.2.42, this parameter is just a function of the Sound Power Level and the distance from the source, hence, characterising this Power one can obtain immediately the Sound Pressure Level at the desired point, and it will show the same behaviour.

The following calculations correspond to Eq.2.36. It describes the sound Power radiated by one side of the plate, and assuming it to be infinite.

The screen of the previous work has the aspect ratio of 140x165 cm. The original plate, which is used at this moment, is made by an expanded plastic, bounded between two paper layers. Hereafter the most important characteristics regarding the foregoing sound radiation and critical frequency are presented:

- Thickness plate: 5mm.
- Density plate: 110 Kg/m^3.
- Young Modulus: 3.456×10^8 N/m^2.

Table 3.1 shows the same parameters for some sample materials. They can be found at [B-C].

Table 3.1   Flexural Stiffness and density for different materials.

Material	Young's Modulus [GPa]	Density [kg/m^3]
Steel	190-210	7850
Glass	72	2400-2800
Concrete	17-31	2300-2400
Aluminium	70	2710
Polyethylene	0.2-0.7	900-950
Polyether foam	0.2-0.5	25-28
Natural Rubber	0.05	920
Polymides	3-5	1140
Polystyrene	2-2.5	1000

Figure 3.1-3.3 shows the Sound Power Level obtained for some of these sample materials. As it is obvious, for an increasing value of the Young

modulus will lead to a decrease in the critical frequency, and the other way around. In the other hand, an increase in the material density gives us a decrease in the Sound Power level. The peak corresponds to the critical frequency, which is higher when the rigidity decreases, according to Eq.2.26.
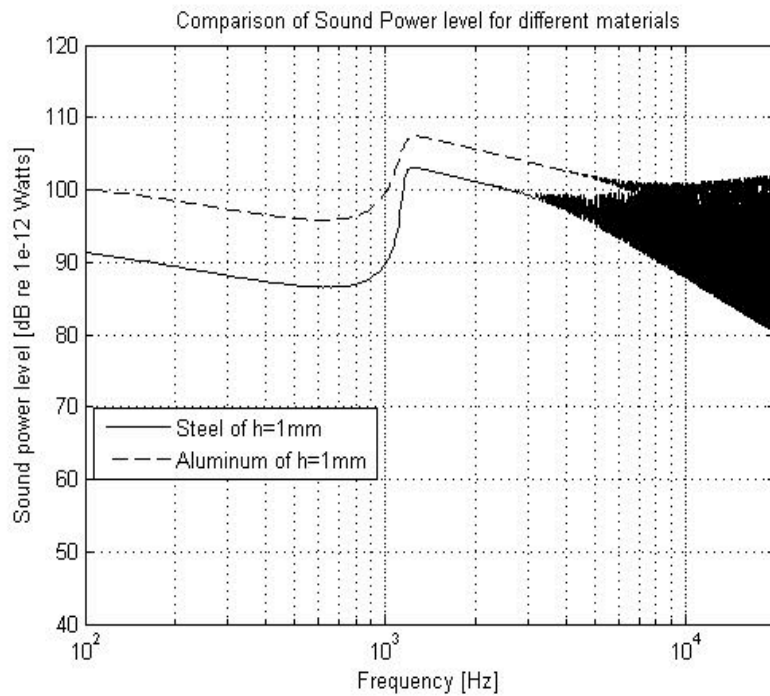
Figure 3.1   Sound power level of a steel and aluminium material.
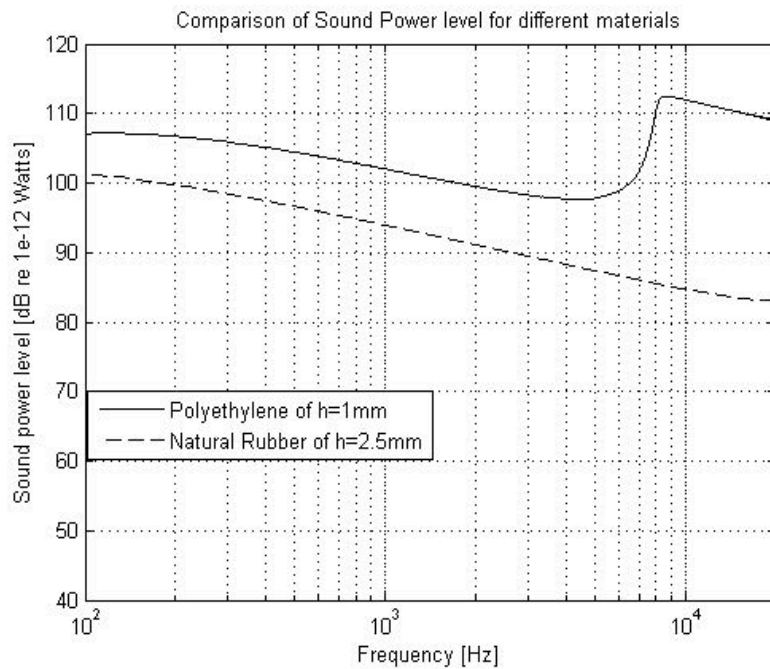
Figure 3.2   Sound power level of a Polyethylene and rubber material.
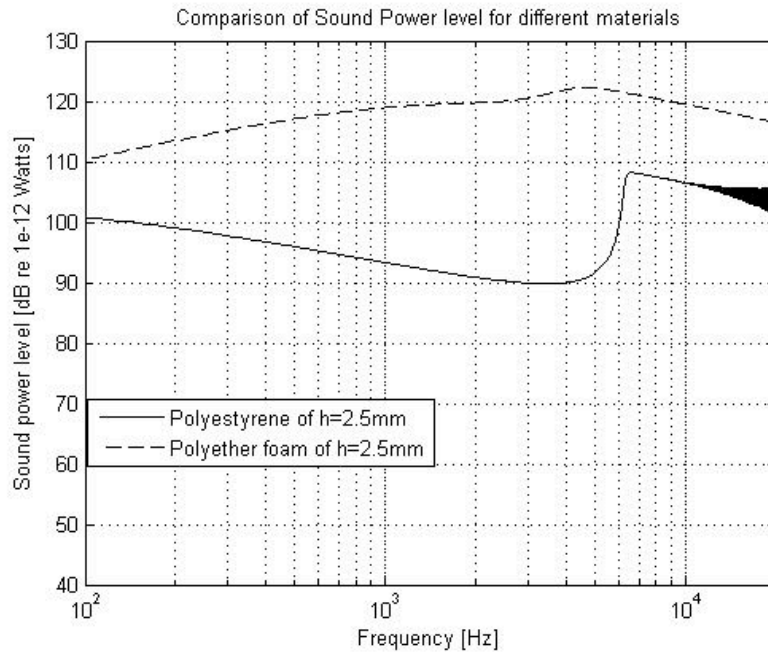
Figure 3.3   *Sound power level of a Polystyrene and foam material.*

These previous figures show up the capital importance of the plate material. As we can see on figure 3.3, the best results can be achieved with thin polyether foam, obtaining pretty flat frequency response. The next figure shows a comparison with the previous structure. An increase in the critical frequency is achieved, as well as higher Power radiation. This is due to the material parameters, as it was discussed before. Furthermore, the frequency response seems to be even flatter.

Another point to consider is the rigidity. If the material is very elastic, it may lead to unwanted vibrations on the plate that will difficult the vision purposes. But, the Elasticity Modulus is around the previous plate, so we don't have to concern about this fact a priori.

For those reasons, a thin, rigid and very light Polyether material will be chosen instead for optimization purposes.
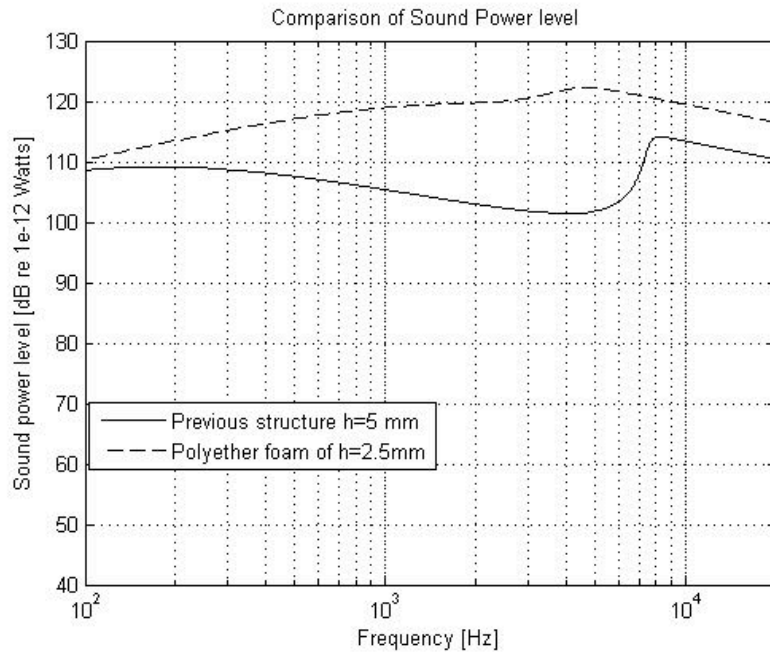
Figure 3.4   Sound power level of the previous structure and polyether foam plate.

Figure 3.5 shows the radiation after the optimization material process, according with Eq.2.46.
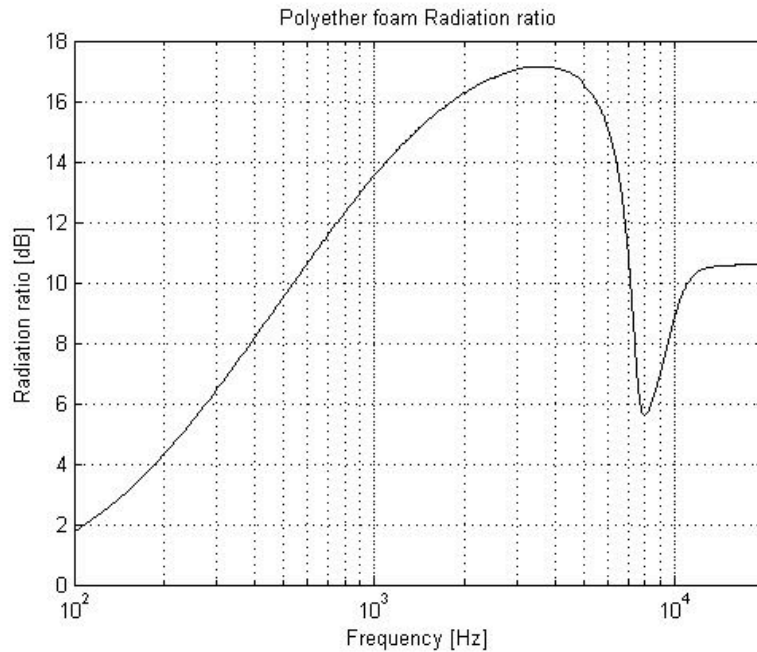
Figure 3.5   Radiation ratio after material optimization

We can see, as it was easily to infer looking at Figure 3.4, that we obtained a big increase in the SPL, since this parameter is higher at all frequencies in the new theoretical structure.

3.2.4 Commercial Materials

As one can find at United States Patent 6031926 [D], the panel is defined as a rigid lightweight panel having a core of a rigid plastics foam e.g. cross linked polyvinylchloride or a cellular matrix, i.e. a honeycomb matrix of metal foil, plastics or the like, with the cells extending transversely to the plane of the panel, and enclosed by opposed skins e.g. of paper, card, plastics or metal foil or sheet. Where the skins are of plastics, they may be reinforced with fibres e.g. of carbon, glass, Kevlar (RTM) or the like in a manner known per se to increase their modulus.

Envisaged core layer materials include fabricated honeycombs or corrugations of aluminium alloy sheet or foil, or Kevlar (RTM), Nomex (RTM), plain or bonded papers, and various synthetic plastics films, as well as expanded or foamed plastics or pulp materials, even aero-gel metals if of suitably low density.

Again, the material that will be chosen depends of the availability of itself.

3.3 Exciter model for Bending Wave Loudspeakers

It is possible to energise, or excite, A BWL in a variety of ways, depending on the application to which the loudspeaker will be put. However, in most cases, a simple electro-dynamic exciter will suffice.

A universal type of exciter can be built around the "inertial" principle [11], this type of exciter has its magnet assembly freely suspended from the panel rather that being fixed as in the bender type. The lower limiting frequency is given by the fundamental resonance between the magnet assembly mass and its suspension stiffness.
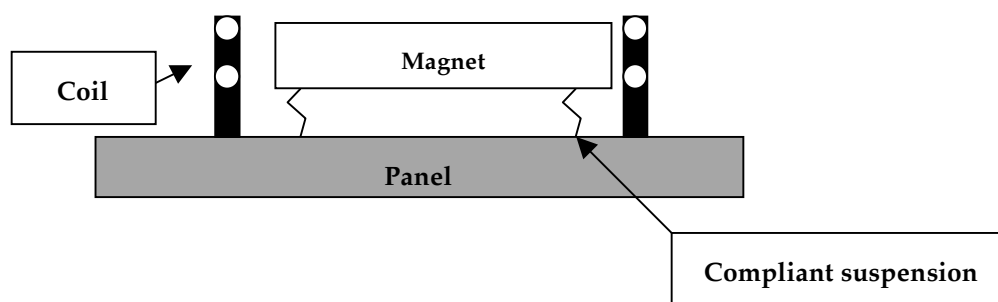
Figure 3.6   *Inertial Type electro-dynamic exciter*

Now it is possible to use standard equivalent circuit analysis techniques to model the behaviour of the combination of exciter and distributed mode panel in the same manner as for conventional loudspeakers. Figure 2.7 shows the

basic mechanical arrangement for a BWL with inertial type exciter which is converted to the equivalent circuit in figure 2.8:
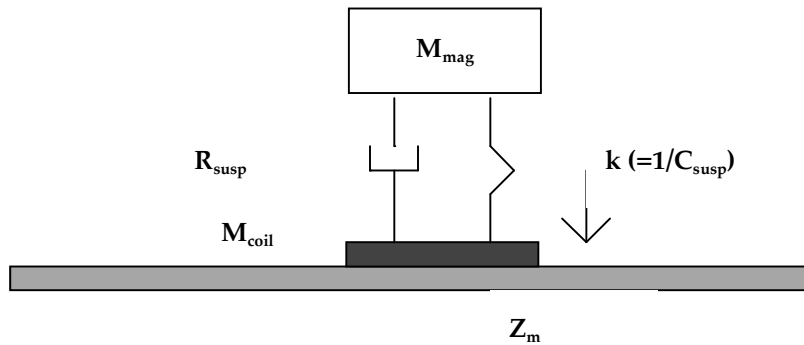
Figure 3.7   *Mechanical analogy of the exciter*
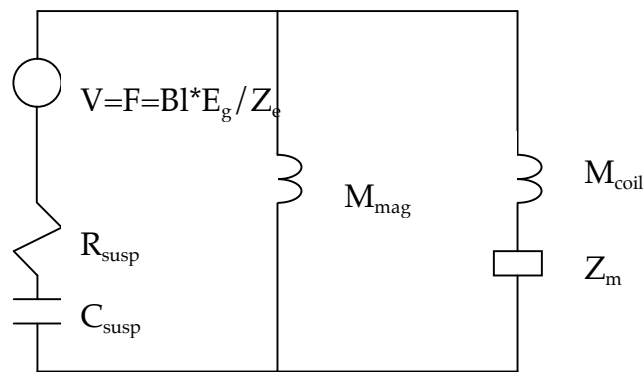
Figure 3.8   *Equivalent Circuit for exciter and panel (impedance analogy)*

Although a full analysis would yield a complex expression for Z_m, in most cases we can approximate its value to being purely resistive with a value given by Eq.2.21.

The diagram above shows us a second-order high-pass filter, and it will therefore be possible to calculate a system fundamental resonance in the same way as for a conventional loudspeaker. The electrical impedance of the exciter and panel combination is given by:

$$Z_e = Z_{coil} + \frac{Bl^2}{Z_{mtot}}$$

(3.1)

After further simplifications, we will lead to the expression below for the total impedance:

$$Z_{tot} = R_{susp} + \frac{1}{j\omega C_{susp}} + \left[\frac{1}{j\omega M_{mag}} + \frac{1}{j\omega M_{coil} + Z_m}\right] \quad \text{with} \quad Z_m = 8 \cdot \sqrt{B'm''} \qquad (3.2)$$

Examining the circuit, one can note that the coil mass appears in series with the panel impedance, and this will contribute to a slight reduction of high frequencies.

Sometimes it is more useful to handle the inverse of the impedance, which is termed mobility, defined as the complex ratio of velocity and force taken at the same point during simple harmonic motion [12]. The use of the mobility usually facilitates the process of evaluating the vibrating structures.

$$Y_{tot} = \frac{v}{F} = \frac{1}{Z_{tot}} \qquad (3.3)$$

The applied force is given by the magnet and voice coil and can be expressed as:

$$F = Bl \cdot \frac{E_g}{Z_e} \qquad (3.4)$$

Since the electro dynamic exciter is a type of moving coil system we can express the high frequency coil impedance as [9]:

$$Z_e = R_e \cdot \left[1 + \frac{\omega}{2\pi f R_e}\right]^{ExpoR_e} + i\left[\omega \cdot L_e\right] \quad \text{Where} \quad r = \frac{1 + ExpoL_e \cdot \left(\frac{\omega L_e}{R_e}\right)^2}{1 + \left(\frac{\omega L_e}{R_e}\right)^2} \qquad (3.5)$$

If we were modelling a mass controlled device such as a conventional moving-coil loudspeaker, we would examine diaphragm acceleration since this is proportional to radiated SPL. A BWL, however, it has instead substantially resistive mechanical impedance, therefore we must inspect the velocity to characterize it.

Figure 3.9 below can be considered as a good indication of the bandwidth available from the BWL, which is approximately 30Hz-20 kHz, more than sufficient for our purposes. A further discussion can be found at [8]. The parameters used have been taken from [11].
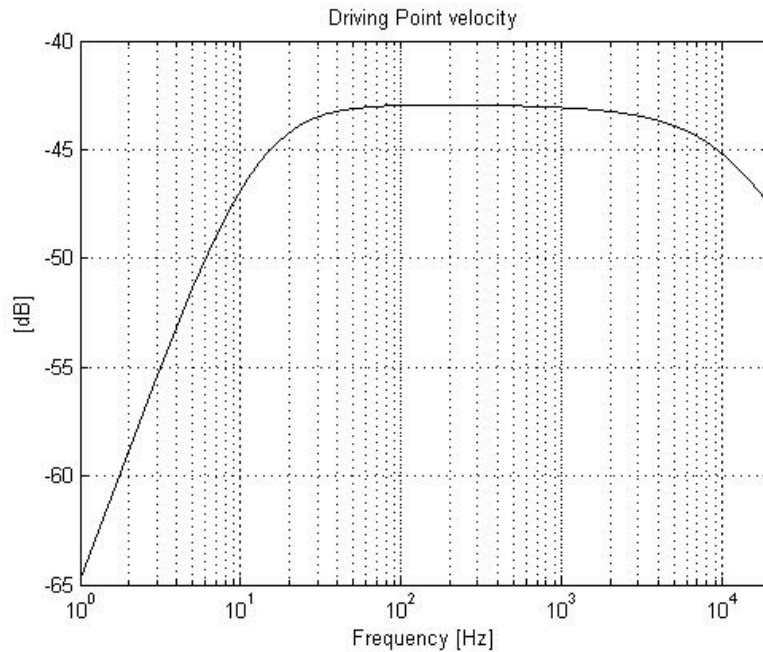
Figure 3.9   Velocity at the driving point for the moving-coil system.

Referring to Figure 3.8, we can see that coil mass is in series with Z_m, and it contributes to a slight decrease in high frequencies. However, due to its almost uniform power in all frequencies, this energy reduction at very high frequencies may prevent the loudspeaker sounding too bright.

Nevertheless, some assumptions have been made that can jeopardize the validity of the model. The most important is the approximation of the panel impedance as a pure resistance. As it is found in [2], only a small error will be introduced, especially at low frequencies.

Moreover, this result assumes a point driving, which is not entirely real. We have a small radius around the exciter. Additionally, no terms for the radiation impedance of the panel have been included.

3.4 Moving-Coil Driving Technology

A new transducer technology has been developed recently by Sonic Impact technologies [F], which can be used as a first driving option for our optimization purposes.

The design-patented by NXT Audio transducers produces high-quality sound when placed against a wide range of materials including glass, plastics, metals, wood, composites and even some fibrous materials.

Figure 3.10   *Sonic Impact NXT driver*

Chapter Four

Material Testing

4.1 Introduction

In order to find the optimum material speaking in terms of sound radiation and frequency response as it was discussed previously; four different sample materials with different thicknesses were tested. Again, we guided our research taking into account the availability of the material.

Moreover, three different driving technologies were tried, according with subsection 3.4.

To perform the measurements, a vibro-acoustics lab was used. With the aid of a Maximum Length Sequence System Analyzer [G], one can measure and analyze many types of linear systems within audio and acoustics area. In addition, the XY-control machine [13] allows us to scan and measure the impulse response of the surface of the bending plate when we excited it using a Sonic-audio [H] driver, (a commercial exciter with NXT driving-based technology).

The MLS technique, in contrast with the well-known white noise FFT analyzers, employs a special type of test signal called maximum-length sequence which is in the other hand deterministic and periodic but retains most of the desirable characteristics of white noise. It measures the impulse response – the most fundamental description of any linear system- from which a wide range of important functions are derived through computer-aided MATLAB® post-processing. The transfer function, which allows us to characterize each material and its sound radiation properties, is obtained by applying an FFT to the impulse response measured [14].

4.2 Set-up

The four plated structures are composed of a kind of polyether foam material, which essentially has the desired characteristics of low weight and rigidness. At this moment, values for the Young modulus or density were not measured or provided by the manufacturer. Three of them have a paper layer covering their surfaces, providing a smooth, bright surface. On the other hand, the last one is just the foregoing material, which may give us a more diffuse sound field. The dimensions are the same in all the samples, being 70x100 cm.
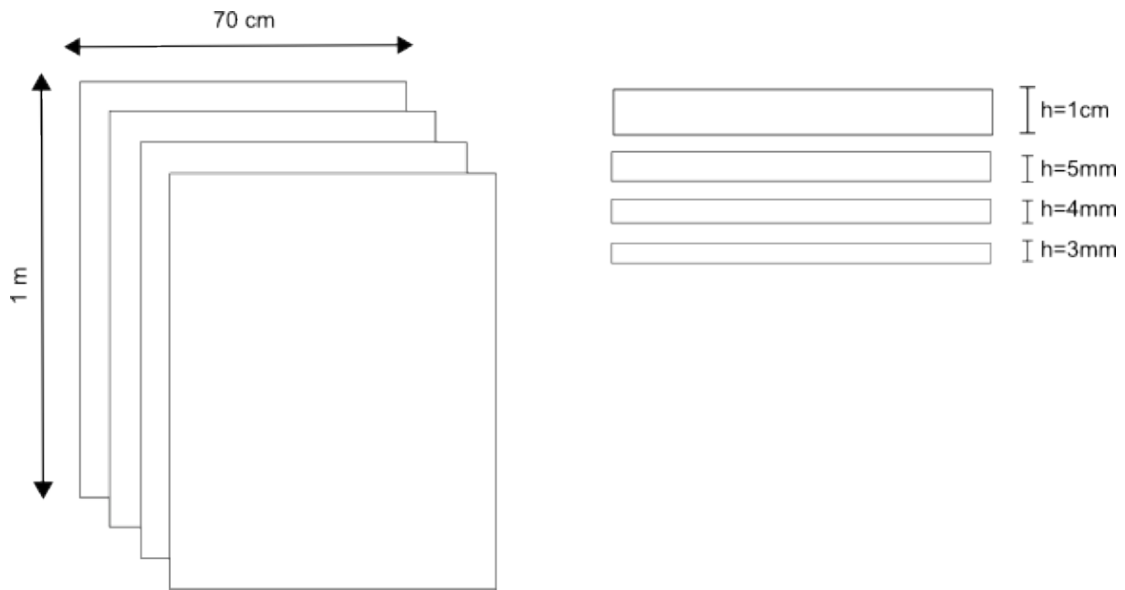
Figure 4.1   *Panel dimensions and thickness*

The MLSSA system was connected by a parallel port to the XY system, which scans the surface and measures the impulse response for each point defined for the control software. The measurement matrix grid was composed by twenty points. An electrets microphone is in charge of collecting the signal provided by the panel, where a Sonic-Impact® exciter is attached on the back center. This exciter is fed by a Yamaha MS-35 Power amplifier, which gives us the sufficient driving power to be ahead of background room noise. Further information about the equipment can be found in Appendix 1.

The panel is hung up over the ceiling with a fish nail. In order to disturb as less as possible the panel behavior, small springs support it on the corners.
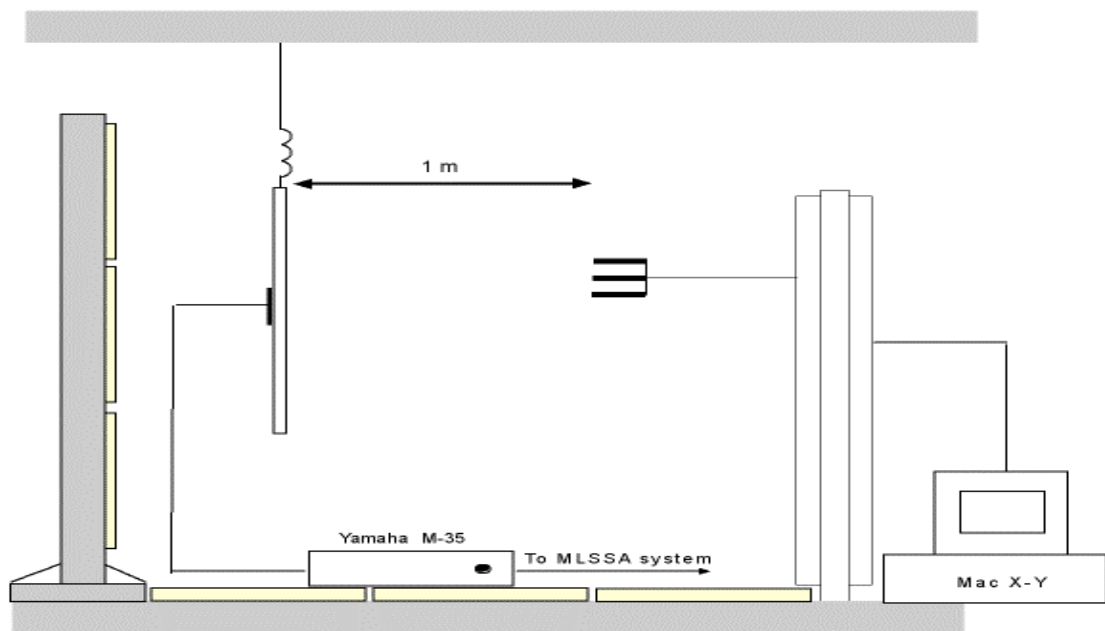
Figure 4.2   *Anechoic measurement set-up.*

Two different approaches were used to obtain the correspondent transfer function: Simulate anechoic measurements and Near-field measurements.

The "anechoic" response of the panel is determined by first measuring the combined room/panel response at 1m and then using the markers to select out only the initial "anechoic" segment of the impulse response, where just the initial transient is taken into account, and therefore no reflections of the room are included. This interval is referred to as the time window. The true frequency resolution using a rectangular time window of T is 1/T, i.e. if T=5ms, the frequency resolution will be then 200Hz. The frequencies below this factor cannot be considered as valid and should be ignored.

As we can see in the anechoic measurements on appendix 2, the true frequency resolution given by the time window is not enough to characterize properly the transfer function in the low frequency range. The room's dimension and its absorption are not sufficiently large to spread and attenuate the reflections from the ceiling and walls, which leads to a short time between the arrival time of the first room reflection relative to the arrival time of the direct sound, and therefore a short time window, which leads to a poor frequency resolution.

On the other hand, one can measure and combine individual points of near field measurement to obtain the correct overall low frequency anechoic panel frequency response. This method was originally proposed in an award winning AES paper [15]. In this case, the microphone is positioned as close as possible to the panel. Near-field loudspeaker measurements correctly predict the true anechoic response only below roughly 4290/d, where *d* is the diameter of the exciter.

Therefore, the resulting frequency response will be a combination of the "anechoic" transfer function for the frequency range above the true frequency resolution, and Near-field measurements in the low frequency range.

4.3 Results and discussion

In this subsection, the transfer functions obtained applying the combined method are presented and discussed for all the sample panels. A comparison with simulation is also given to verify that this model is accurate and it can be taken into account.

Figures 4.3-4.6 show the transfer function for each structure.
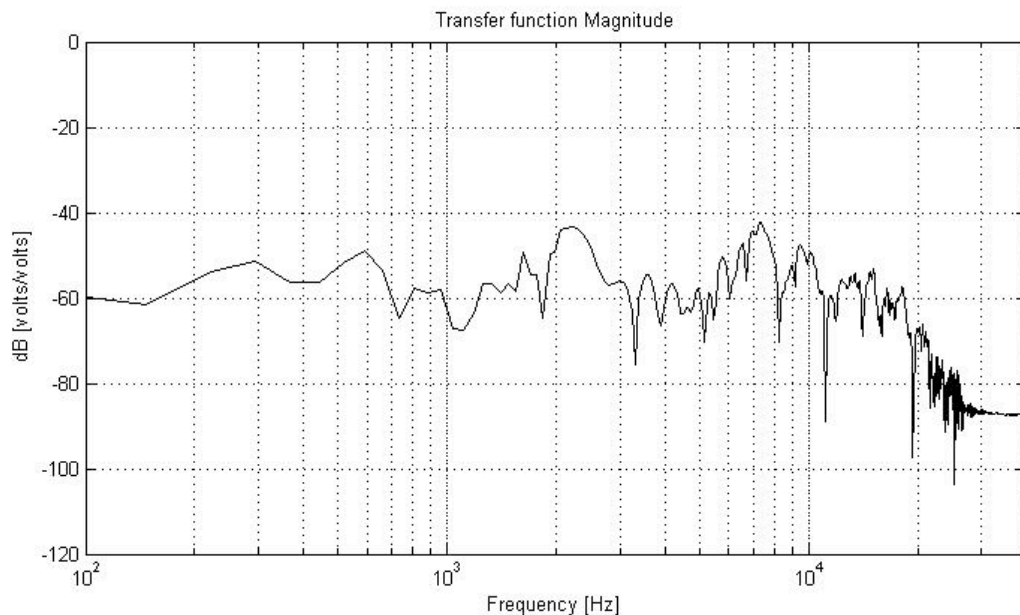
Figure 4.3   *Transfer function magnitude for Polyether foam with and attached paper of h=0.3 cm*
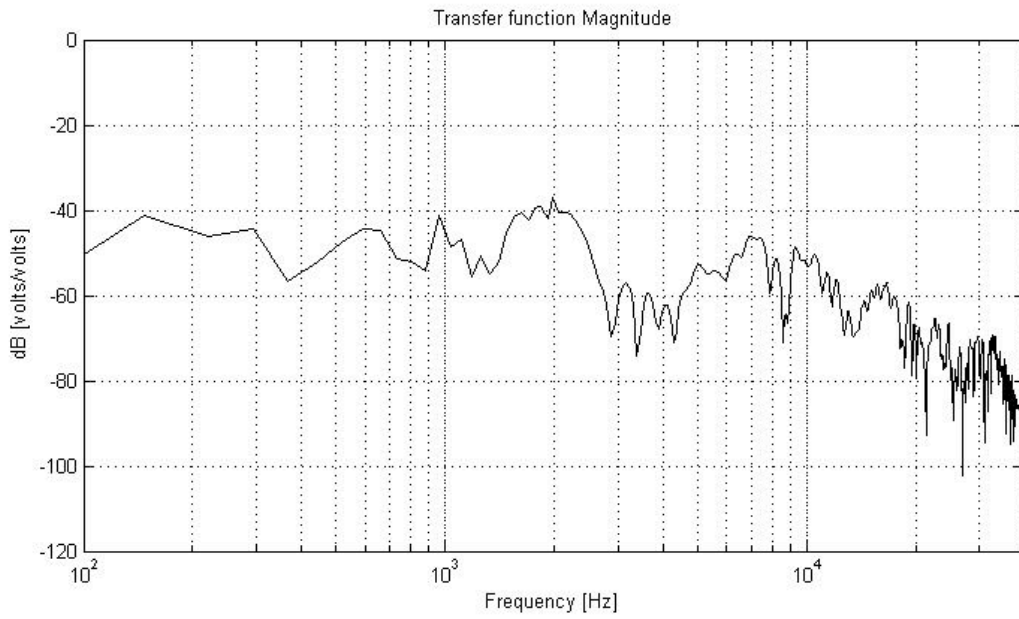
Figure 4.4   Transfer function magnitude for Polyether foam of h=0.4 cm
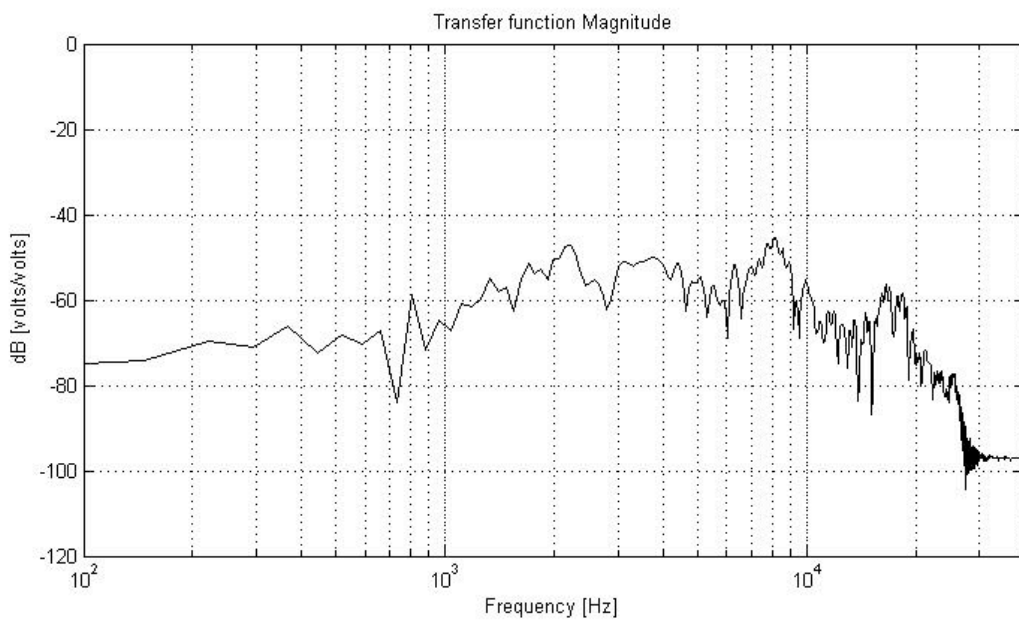
Figure 4.5   Transfer function magnitude for Polyether foam with and attached paper of h=0.5 cm
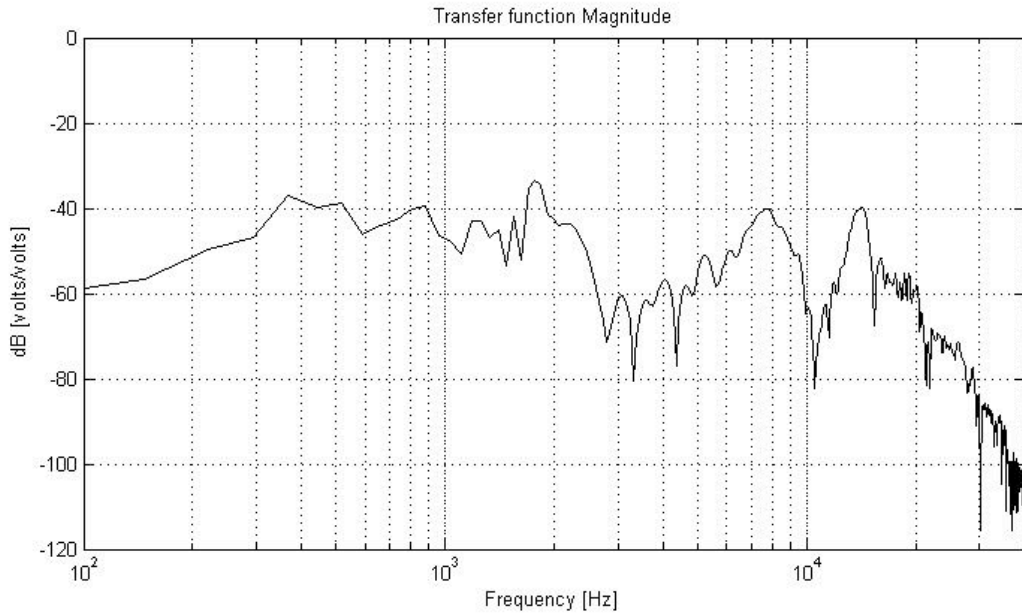
Figure 4.6   *Transfer function magnitude for Polyether foam with and attached paper of h=1 cm*

Analyzing the results, we can infer that the measured transfer functions compares well with the analytical solution given by Eq.2.36. As we said, the Sound Power Level, and therefore the Transfer Function follows approximately the model of subsection 3.2.3.

The following plot shows the foregoing comparison between the model and the measured transfer function for h=3mm. We must say that they fit each other reasonably well, so the model can be considered a good approximation to the real behaviour. The slight decrease at high frequencies in the measured function may be due to the load of the coil exciter. When a small area is used to drive the panel instead of a point source, then the diameter of the drive patch will decrease the response at high frequencies.
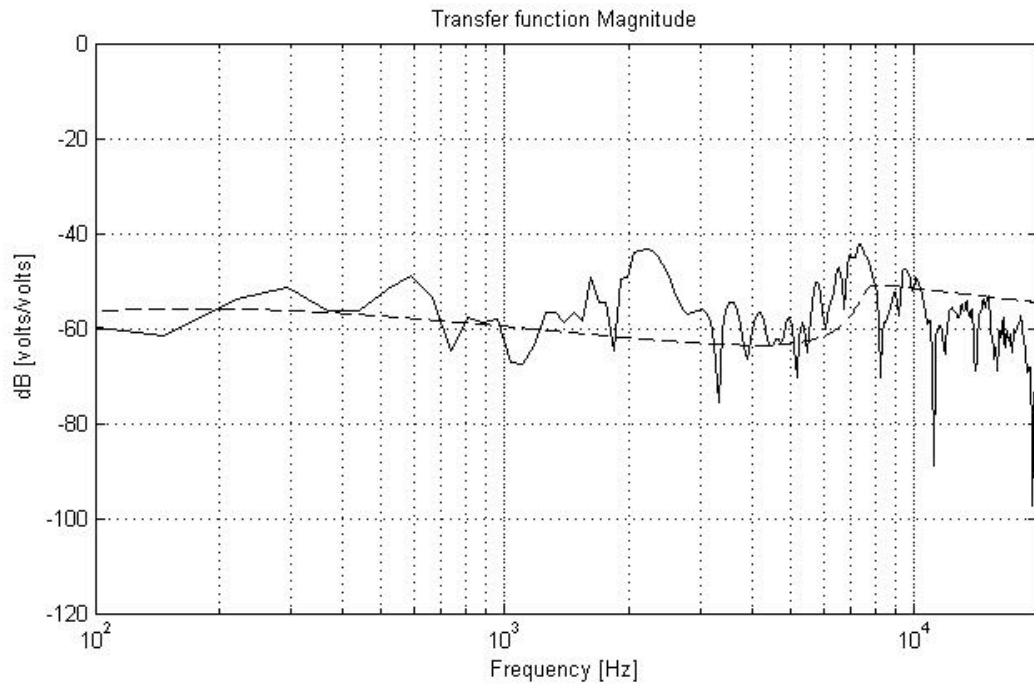
Figure 4.7   Measured and calculated Transfer Function comparison.

For an increasing thickness, the transfer function gives us lower values, due to the quadratic inverse relation between m'' and SPL, related by Eq.2.37

Moreover, the frequency response becomes rougher when the thickness increases, which can be due to a decrease in the critical frequency, since we can just consider valid the results of Eq.2.36 when $f \ll f_c$.

In all the plots we can see a peak in about 2300Hz. This is probably due to some exciter resonance. It also appears in the previous structure, whose transfer function can be seen on Appendix B. The manufacturer does not provide any further information.

For these reasons, the best choice can be the polyether foam material with thickness=3mm. It provides the flattest and the highest Transfer Function for the same set-up conditions.

Since our aim is to drive the panel below the critical frequency about f_c 15kHz, we must characterize it, which cannot be observed just by looking at the transfer function. Therefore, we will measure the Young modulus for the two different samples material and the critical frequency will be obtained.

4.4 Panel mechanical measurements

4.4.1 Young Modulus measurement

In order to find if we can achieve the desired critical frequency with the available materials, measurement of Young Modulus is required. This can be done by the Complex modulus apparatus 3930, provided by Brüel&Kjaer. The apparatus is composed of two Magnetic Transducers MM0002, one Capacitive Transducer Type MM0004, and a special test jig which provides firm clamping of the samples with very low parasite losses, and precise mounting of the transducers with respect to the sample [16].

A bar shaped material sample is clamped at one end. The electronic equipment consists of an MLS sequence driving the exciting transducer and an amplifier to amplify the signal picked up by the pick-up transducer. Samples cut from non-magnetic materials have to be made susceptible to magnetic fields by fastening a small ferro-magnetic disc. Photograph of the set-up is included in Appendix C.

Young Modulus is determined by reading the resonant frequency f_n on the transfer function measured and measuring the constants of the sample bar, following the expression:

$$E = 48 \cdot \pi \cdot \rho \left(\frac{l^2}{h} \cdot \frac{f_n}{k_n} \right) \qquad \text{Dyne/cm2} \tag{4.1}$$

Where l is the free length, h the thickness, the density in g/cm^3, and k_n the coefficient given by table 1 in [16].
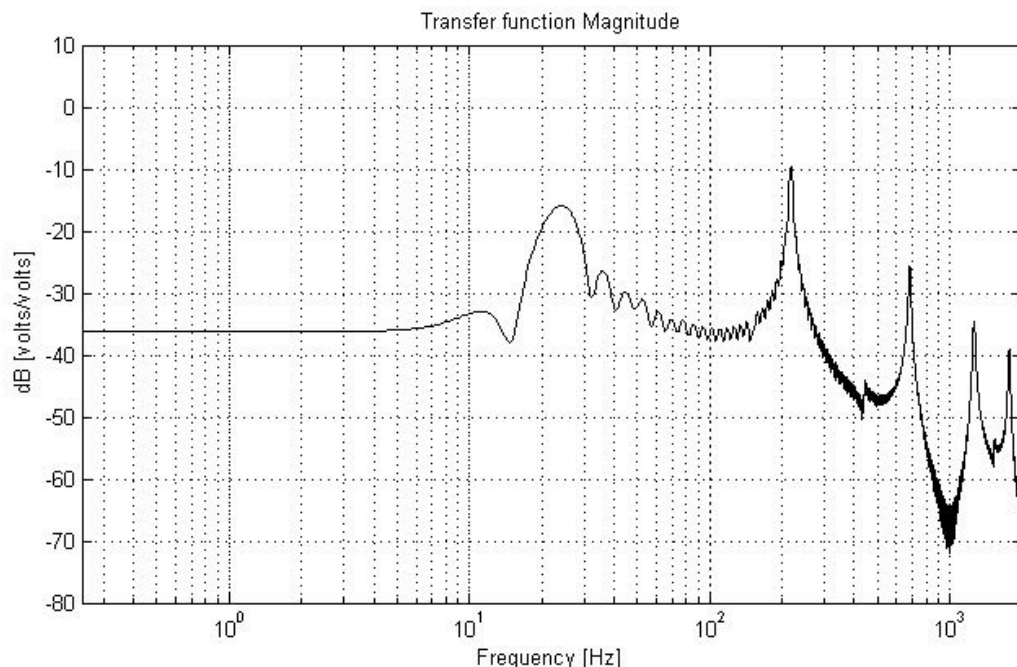
Figure 4.8   Transfer function magnitude of paper foam as a function of frequency.

The resonant frequencies were found by Matlab® processing, and the material constants for the two different samples were measured:

Table 4.1 *Material parameters*

	Sandwich material	**Polyether foam**
Density	$0.11 \text{ g}/\text{cm}^2$	$0.08 \text{ g}/\text{cm}^2$
Length	18.3 cm	22.1 cm
Thickness	0.5 cm	0.4 cm
2nd Resonance freq.	218 Hz	80 Hz
k_2 value	22	22

The equation above gives us the value for the modulus of elasticity *E* of the sandwich material and polyether foam material:

$$E = 2.296 \cdot 10^8 \, {N}/{m^2} \qquad\qquad E = 7.47 \cdot 10^7 \, {N}/{m^2}$$

Inserting it into Eq.2.5 and 2.26, it yields to the following critical frequencies for the different structures.

Table 4.2 *Critical frequency for different sample materials.*

	Critical frequency
Polyether sandwich of h = 0. 3 cm	$f_c = 17379$ Hz
Polyether foam of h=0.4 cm	$f_c = 16007$ Hz
Polyether sandwich of h= 0. 5 cm	$f_c = 8566$ Hz
Polyether sandwich of h= 1 cm	$f_c = 4083$ Hz
Previous structure h=0.5 cm	$f_c = 6981$ Hz

As we expected looking at foregoing equations, the thickness takes a capital role defining critical frequency. This parameter modifies the stiffness-mass per length ratio, lessening it when the thickness decreases, since there is an inverse relation between them.

Furthermore, comparing with the previous structure, a substantial critical frequency increase can be achieved. Indeed, all the sound power will be

radiated by the near-field in the range of interest, which means that higher diffuse field is obtained.

We can conclude then that for our optimization purposes, polyether foam of thickness h=0.3 cm will be chosen instead.

4.4.2 Determination of the mechanical impedance

In order to characterize and validate the vibrating panel with the theoretical model, the mechanical impedance was measured, both for the damped and the un-damped plate. Ideally, the mechanical impedance of the un-damped plate should show the panel modality, while the resonances and anti-resonances of the modes in the damped plate should be strongly attenuated, due to the quasi-infinite behaviour of the damped panel.

It is possible to use a direct dynamic measurement of the panel mechanical impedance with an impedance head. Two transducers are used together. A force transducer measures the force applied to the panel, and an accelerometer measures the movement of the panel. The transfer function of force/velocity is directly related to the mechanical impedance. Both outputs are charge, which is therefore conditioned by a charge amplifier that filters and amplifies the charge from a transducer to a voltage signal output that can be acquired by the VXI acquisition station, which comprises the FFT analyser. The transfer function is therefore:

$$T(\omega) = \frac{Force(\omega)}{Acceleration(\omega)} \tag{4.2}$$

However, the force measured by the force transducer is not the true force, bus has added to it the inertial forces of the sensing tip. This force needs to be subtracted when calculating the mechanical impedance:

$$Force_{true} = Force(\omega) - m \cdot a(\omega) \tag{4.3}$$

Where m is the mass of the sensing tip. The velocity is found from the acceleration by scaling by j -method.

$$Velocity(\omega) = \frac{a(\omega)}{i\omega} \tag{4.4}$$

Finally the mechanical impedance is therefore obtained:

$$Z_m = \frac{i\omega[f(\omega) - m \cdot a(\omega)]}{a(\omega)} \tag{4.5}$$
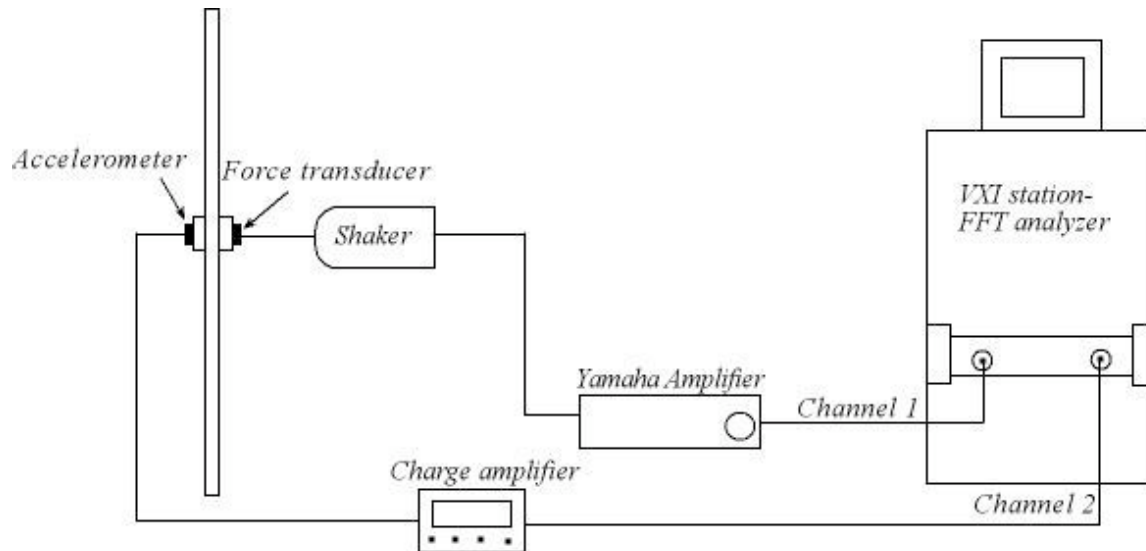
Figure 4.9   Schematic for impedance measurement set-up.

The mechanical impedance can easily be obtained from a measurement of the transfer function and knowledge of the tip mass, which can be seen at the calibration chart of the transducer.

The tip mass also determines the upper frequency limit of the measurement. When the inertial forces of the tip are comparable to the forces of interest, then it becomes progressively more difficult to extract the true force from the combined force. An estimate of the upper frequency limit is given by:

$$F_{upper} = 2\frac{Z_m}{m} \hspace{4cm} (4.6)$$

Figure 4.10 illustrate the comparison of the measured mechanical impedance of the chosen panel and the theoretical value for the same panel obtained by Equation 2.21.
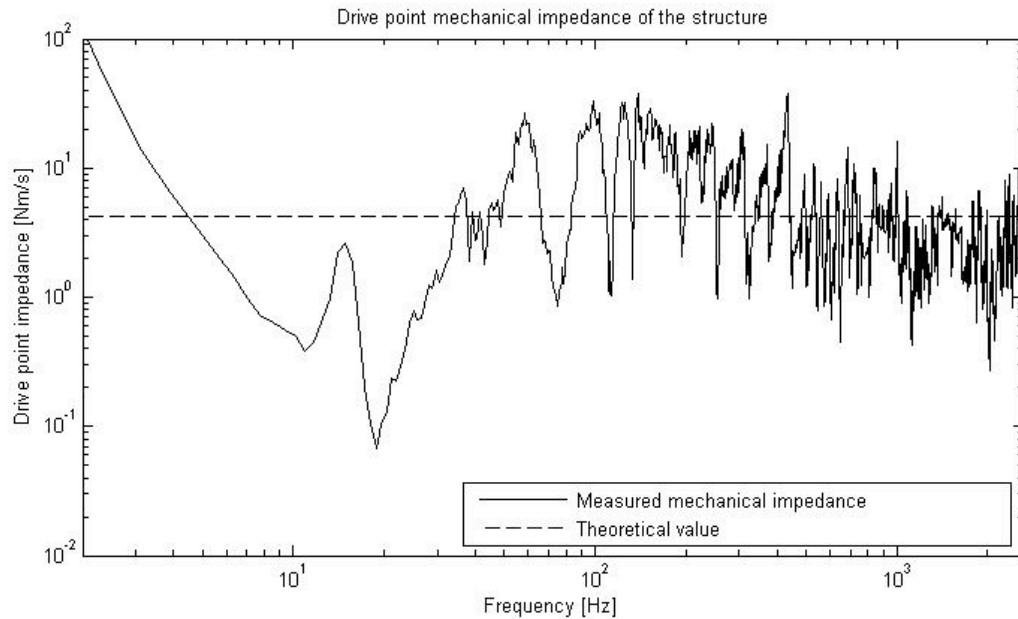
Figure 4.10 *Comparison between measured mechanical impedance and infinite impedance at the drive point up to F$_{upper}$.*

Analysing the graphic, we can see that although the measured mechanical impedance shows the panel modality in the resonance and anti-resonance peaks, the value of the impedance settles to that of the infinite plate. This confirms that the value for an infinite plate can be conveniently used as the load for the electrical equivalent circuit, and it is a good approximation of the real value. Furthermore, in the very low frequency range we can see the expected compliance control, due to the suspension of the exciter.

This measurement has an upper frequency limit, and it is only accurate up to about 2500 Hz, due to the finite size and effective mass at the measuring point. The measured impedance compares well with the analytical solution, since it is taken over a small area.

4.5 Driving Alternatives Transfer Function Measurements

4.5.1 Introduction

Usually, Bending Wave Loudspeakers and DM loudspeakers are drived by the popular NXT-patented technology, which essentially consists of a magnet-voice coil system. Such an exciter works on the same principle as an ordinary moving coil loudspeaker.

But, however, it is possible to energise, or excite, a DML in a variety of ways, depending on the application to which the loudspeaker will be put. Especially in the last years, when the DML established more and more, the development of exciters increased rapidly. These different exciters vary in size, mass and working principle, as well as in the efficiency of sound radiation.

In the purpose of the work, it is important that the mass of the exciter is as low as possible, for several reasons: to attenuate the reduction at high frequencies due to coil mass and to reduce the load of the panel.

Therefore, a brass exciter and a piezoelectric driver were tested. The circle brass driver has an extremely low mass, with theoretically will give us a better response at high frequencies. The piezoelectric exciter, due to its momentum working principle might minimize the interaction between the two line exciters, which possibly allow us to remove the damping material between lines.

4.5.2 Results and discussion

In this subsection, the results of the measurements that were performed will be presented. In order to keep this section reasonably long, we will show the best results for each driver. The results for the other panels are included at Appendix B.
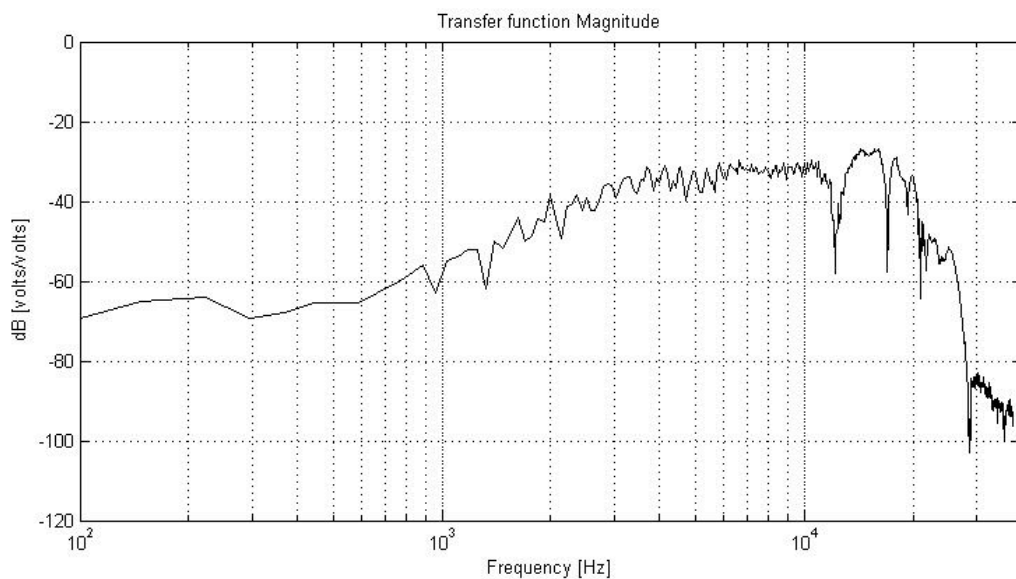
Figure 4.11   Transfer Function Magnitude for the brass exciter, panel of 0.5cm
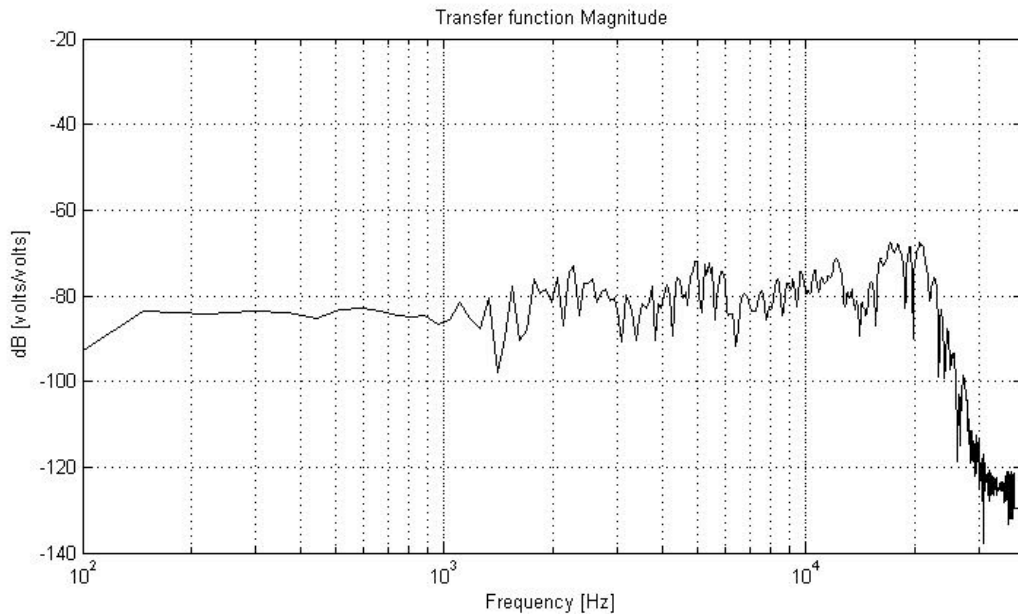
Figure 4.11 Transfer Function Magnitude for the piezoelectric exciter, panel of 0.3 cm

As we can infer looking at the results, the piezoelectric driver turns into a perfectly valid driving alternative. We must say that the results are surprisingly good, achieving a considerable flat frequency response at almost every single frequency. Moreover, the NXT exciter resonance is strongly attenuated. The decay at high frequencies starts in about 20 kHz, which is more than sufficient for our purposes.

As we said, due to the extremely low mass loading, the slight decay at high frequencies cannot be considered.

The main drawback is the lower Transfer Function level comparing with the NXT transducer. This could be a great disadvantage in sound reinforcement and PA systems [18], but, since our aim is to set the loudspeaker 1.5 meter from the listener position, it doesn't seem to be so critic. Moreover, this level will be increased in about 10 dB when we drive the panel with a line, due to the quasi-cylindrical spreading.

The brass exciter provides us a higher level, and it also get rid of the NXT exciter resonance, showing a pretty flat frequency response as well. Nevertheless, there is a reduction in radiation of about 20dB at low frequencies, so it will be disregarded.

So, as a conclusion of all the material testing that has been carried out, we may say that a panel of thickness h = 0.3cm allow us to work at the desired frequency range, and a piezoelectric driver gives us the best features in terms of sound radiation.

Chapter Five

Performing the Loudspeaker

5.1 Introduction

At this point, the best material and driving technology have been selected.

This chapter will be focused on the construction and design of the final vibrating panel.

The first part will explain the loudspeaker set-up, where our aim is to build a Stereo Dipole system for the virtual reality environment.

Secondly, the damping properties and configuration that will allow us to simulate the desired infinite plate will be established.

To conclude, the line-shaped excitation will be constructed by a row of piezoelectric drivers, and finally, the Transfer Function will be analyzed and presented. The loudspeaker will be settled on our virtual reality environment, where the panel would act as passive screen at the same time.

5.2 The Bending Wave Line Stereo Dipole – Final Application

The final aim of the loudspeaker that has been designed is to provide the sound radiation acting as a "Stereo Dipole" that can simulate virtual images around a single listener position for virtual reality applications. Moreover, the loudspeaker will act as a passive screen where images can be projected.

To understand it in a global point of view, it would be necessary to explain what means "Stereo Dipole" and its features and applications.

Hamada's researches [19] demonstrated that a system comprising only two closely spaced loudspeakers can create very convincing virtual images around a single listener. Under certain circumstances, it is possible to give a listener the impression that there is a sound source, referred to as a "virtual source", at a given position in space where no real sound source exists. One way to achieve this is to ensure that the sound pressures that are reproduced at the listener's ears are the same as the sound pressures that would have been produced there by a real source at the same position as the virtual source.

In practice, however, it is advantageous that the desired signals be reproduced accurately not only at the listener's ears, but also in the vicinity of those two points since this will allow moderate head movement without letting the illusion of the virtual image break down.

Hamada showed that the area which the sound field can be controlled is larger when the two loudspeakers are close together. So, reducing the

loudspeaker span into about 10°, we may improve the system's robustness with respect to head movement.

The geometry and solution of the problem can be found at [19]. We can say here that to implement a virtual source there are two main ways: Crosstalk cancellation and Virtual source imaging. Both can be implemented by Digital Signal Processing adding a variable gain and a positive delay corresponding to the time it takes the sound to travel the path length difference.
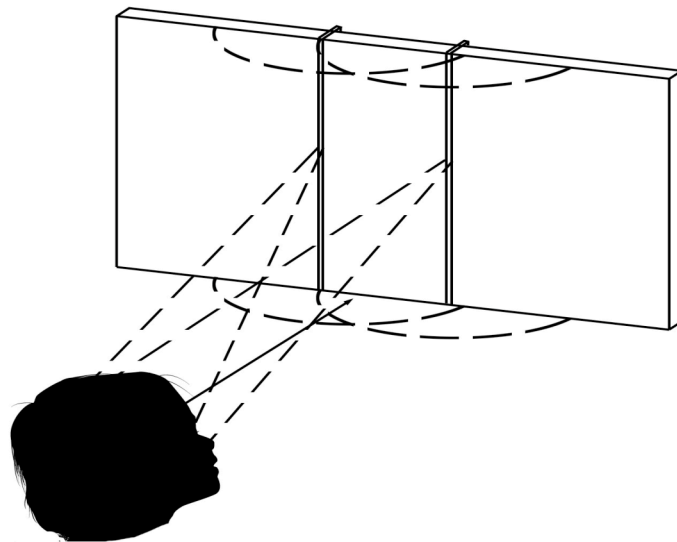
Figure 5.1   *Picture showing the final configuration*

The foregoing plot illustrates the final configuration, where an "optimized" panel, in terms of critical frequency and sound radiation will provide the sound towards the listener. This radiation is provided by two lines of piezoelectric sensors, giving us a pseudo-cylindrical wave front, increasing the sound level and the degree of freedom of the head in the vertical direction.

That listener will be sit 1.3 meters away from the sound source, and the lines are separated 10° from respect to the listener position acting as the mentioned "Stereo Dipole". As we said, the bending wave panel will act as a passive screen at the same time.

So, combining the passive screen and the virtual source imaging we can simulate virtual reality environments. The design of the DSP depends on the desired application.

5.3 Simulating an Infinite Plate - Damping

As we stated before, the Damping mechanism will allow us to modify the behaviour of the plate, eliminating the unwanted reflections at the edges and boundaries, so the plate can be finally seen as an infinite structure which vibrates freely instead of a superposition of modes.

In our damping mechanism, we will follow the Manger transducer principle, where the edges are covered by a star-shaped damping material. The waves will therefore be absorbed and no reflection will stand.

Swedac Acoustic [H] supports our work providing us some of their damping samples and helping us to select the optimum material.

Finally we used two layers of viscoelastic damping layer DG A2, which gives us an averaged lost factor around 0.2-0.3. Usually a lost factor of 0.1-0.2 is sufficient for our purposes.

The next picture shows the final appearance of the loudspeaker. As we can see, the damping layer includes a thin metal foil to constrain it, since it can improve the response for wide frequency range applications.
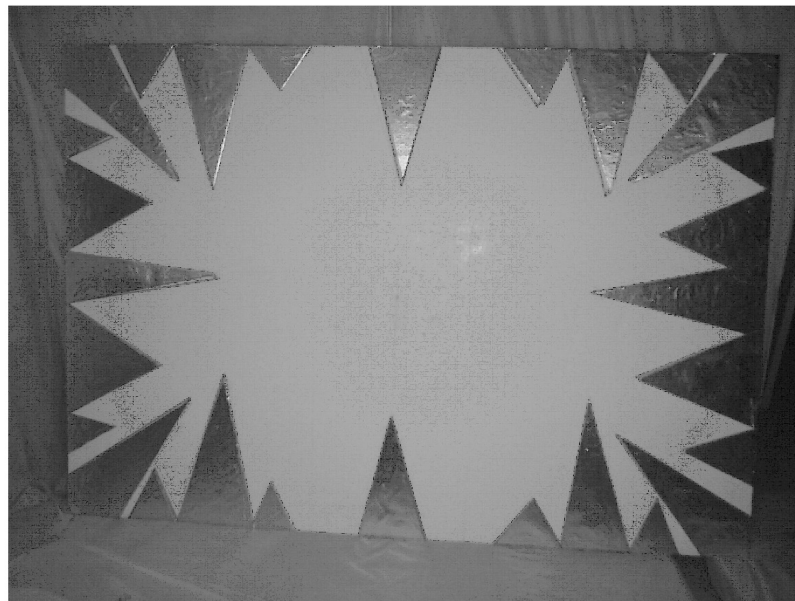
Figure 5.2   *Loudspeaker with Damping layer.*

To probe if the damping mechanism worked in the desired way, we performed two different tests:

- Finite Element Modelling.
- Mechanical Impedance Measurement.

In the first case, we modelled the vibrating surface of the plate by Finite Element Modelling for both cases, un-damped and damped plate. Ideally, the un-damped plate should show the modal distribution, since the oncoming waves are still acting. Adding a damping structure with the same lost factor that the material used, we can see theoretically how the vibration pattern changes to a "quasi-infinite" structure.
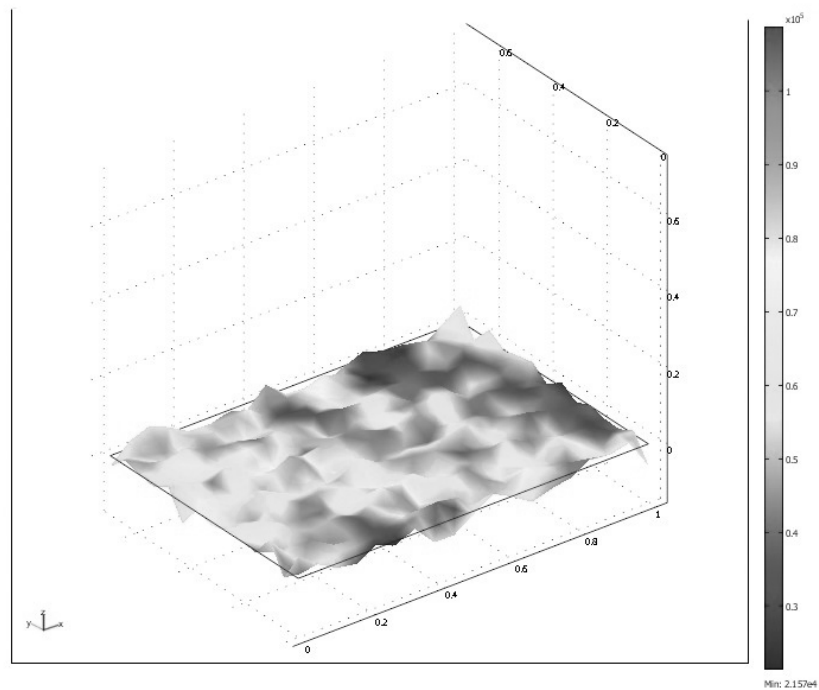
Figure 5.3   Vibration pattern of the un-damped structure.
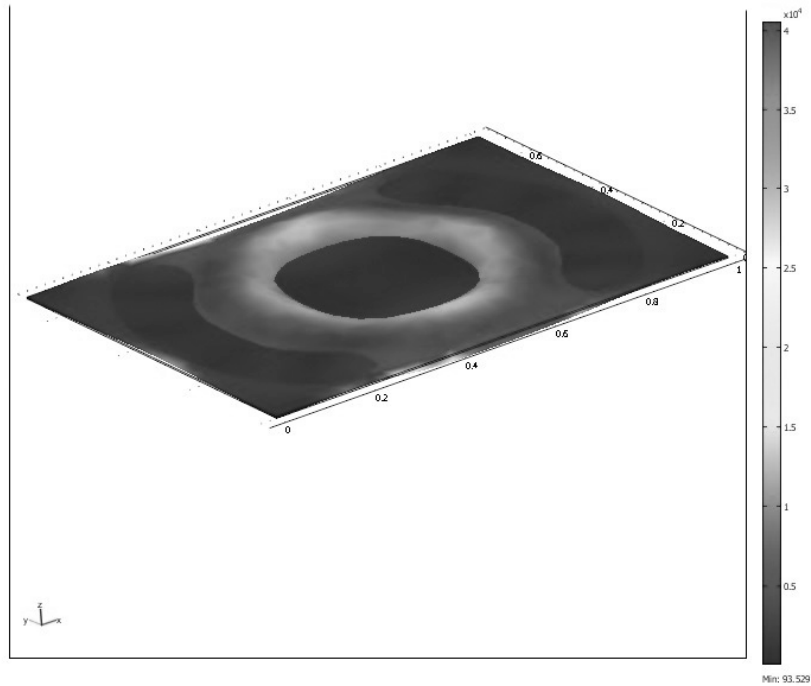
Figure 5.4   *Vibration pattern of the damped structure.*

As we can see in the previous plots, the vibration of the un-damped structure shows the expected random behaviour, since there is still modes acting on the surface and superimposing each other. Moreover, stronger radiation is achieved due to the foregoing superposition.

Otherwise, for the damped plate, lower radiation is obtained, since the most of the waves are absorbed by the damping mechanism. But, the radiation pattern show almost perfect spherical movement. Hence, looking at the FEM result, we can say that the damping mechanism seems to work in the desired way.

But we haven't test the behaviour in the real structure yet, since the FEM just gives us a computer simulation. So, measuring the mechanical impedance measurement we can determine the damping performance. As we explained at subsection 4.4.2, the mechanical impedance of the un-damped plate should show the panel modality, while the resonances and anti-resonances of the modes in the damped plate should be strongly attenuated, due to the quasi-infinite behaviour of the damped panel. The same set-up was used, and the result is plotted in the following figure.
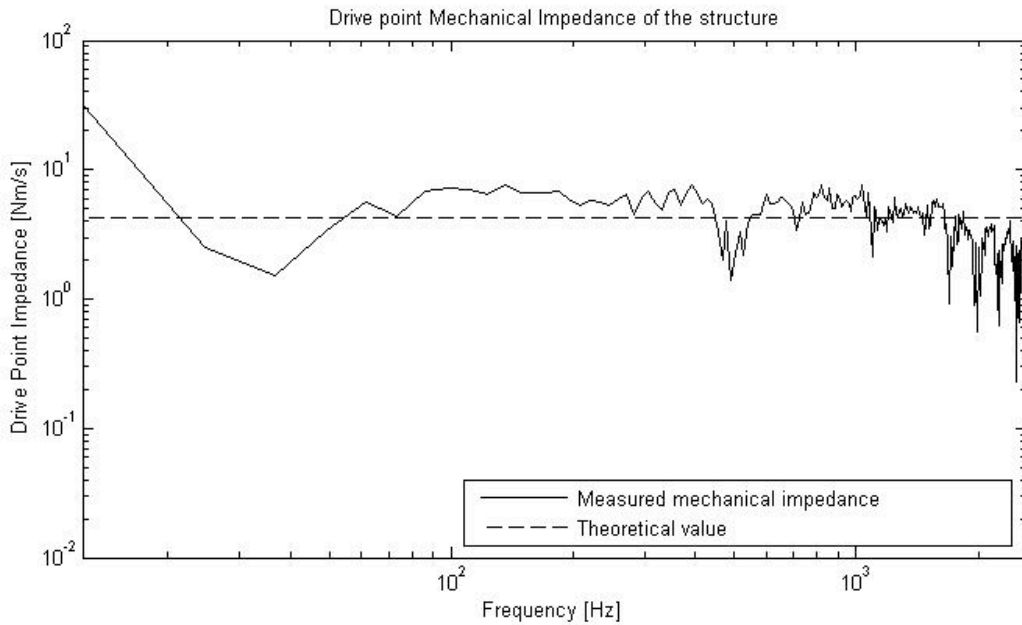
Figure 5.5   *Drive point mechanical impedance of the Damped plate.*

Comparing with figure 4.10, we can easily see how the resonances are strongly attenuated by the damping layer actuation, so both tests gives positive results, and therefore we can rely that an infinite structure was achieved.

5.4 Line Shaped Stereo System

After adding the damping mechanism, the line of piezoelectric sensors was built. Since we need special high-voltage amplifiers to drive the line and we had just one available at the department, just one line of twenty piezo-sensors was attached and measured. The next picture shows the final appearance of the panel, where another line should be attached on the other side. The FEM shows also how the "pseudo-cylindrical" wave front looks like.
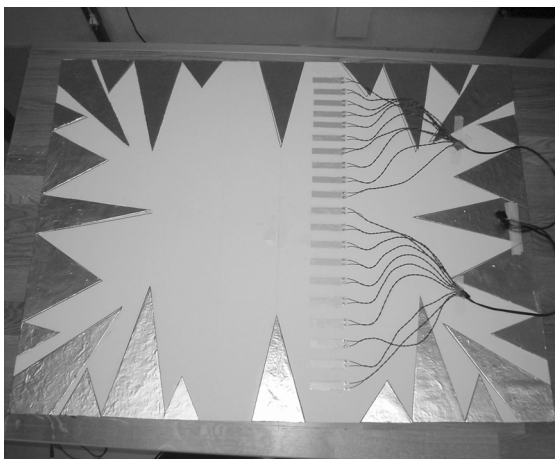
The next plot shows the Transfer function for the final configuration.
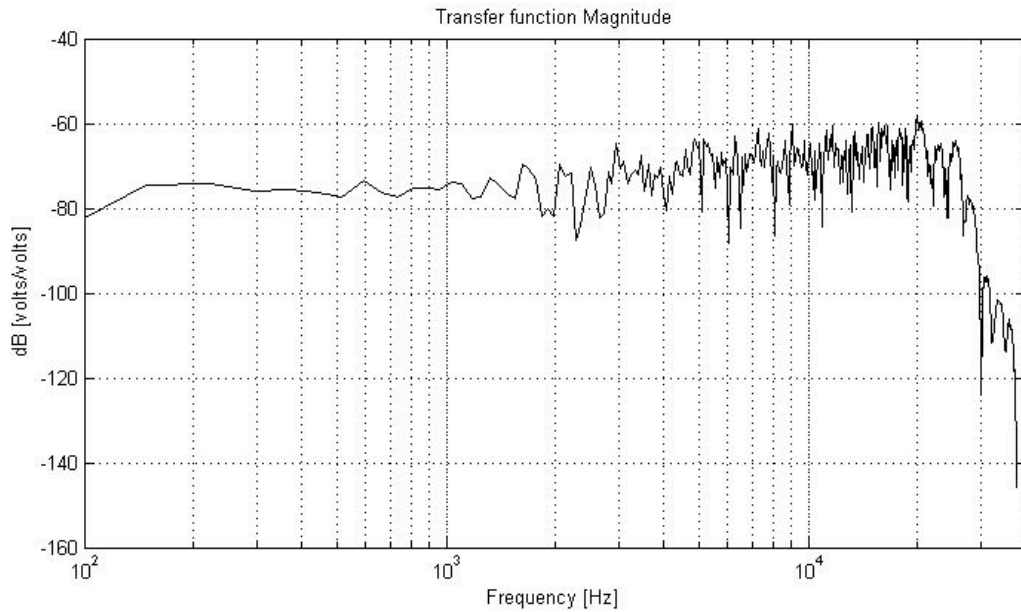
Figure 5.7   Transfer Function magnitude for piezo-line exciter, panel of h=0.3 cm

As we can see, it keeps essentially the valuable flat frequency response, with an increase of about 8-12 dB due to the piezo-line excitation, giving us higher values at every frequency.

Another feature is that, when we measured the near-field scanning in the vertical direction, the Transfer Function doesn't vary noticeable, so we can consider a sort of cylindrical spreading in the vertical direction.

Another important fact is that we obtained lower values at low frequencies. Usually, when we drive a structure with an array of exciters, better low frequency response is achieved. Again, the decay starts over 20 kHz, which allows us to work in the whole audio range.

We had no more time when the work had to be ready, and this fact should be investigated further.

Chapter Six

Conclusions and further procedures

The main objective of this thesis work was to build an optimized bending wave panel in terms of sound radiation and critical frequency. Moreover, a line-shaped piezoelectric exciter is responsible for the pseudo-cylindrical wave front of the structure. As we explained before, our final aim was to build a "Stereo Dipole" where virtual images can be created around a single listener using Digital Signal Post-Processing.

The radiation of sound from vibrating panels appeared very dependant of the material properties of the plate, such as density, rigidity and thickness. Therefore, as it was showed, a very light and thin material has to be used.

After finding the best solution in theoretical terms, some sample materials were tested. As we inferred, the thinnest one gave us the highest value in terms of critical frequency, and its Transfer Function appeared reasonably flat.

Three different excitation methods were tested, and we found that a piezoelectric film can be considered as a perfectly valid alternative, with a pretty flat Transfer Function and very low mass, which reduces the load of the panel. Moreover, due to its momentum working principle, no damping might be needed between lines to keep the infinite behavior, since the interaction between them is almost neglected and it can be disregarded.

Finally, the whole structure was built, with a damping layer attached on the top to provide the desired infinite behavior. As we saw, the performance of the damping seems to be good. Its transfer function was measured, showing again a pretty flat response.

Our last aim was to build the two stereo lines, and measure the combination of Transfer Function and Sound pressure level from the listener's position. Since we had shipping problems during the time of the procedure, and only had one High-voltage amplifier available, the experiment could not be carried out. Thus, the results are just due to one line of piezoelectric sensors. The response of this system can be analyzed further.

Hence, future steps of the work may concern the stereo system. Another line has to be attached, and its combined Transfer function should be measured and analyzed. It would be interesting to investigate if any damping should be added between lines to keep the infinite behavior.

When both lines will be ready, it would be necessary to identify and solve the "Stereo Dipole" problem, using either Crosstalk cancellation or Virtual Image sourcing for the specific application where the panel would like to be settled. Some psycho-acoustics test can be done to see if the panel can be reliable as a "Stereo Dipole" source.

As we tested, the panel can act as a passive screen, but the size might not be properly selected. Therefore, if the system seems to work fine, it would be nice to re-build the system in a bigger panel.

References

[1] Fahy, F., Sound and structural Vibration, Radiation, Transmission and Response, Institute of Sound and Vibration Research, University Southampton

[2] Cremer, L., Heckl, M., Structure Borne Sound, Springer- Verlag, Berlin 1973

[3] Kropp, W., Technical Acoustic 1, Department of Applied Acoustics, Chalmers University of Technology 2002

[4] Elling, W., Acustica 4. 1954

[5] Rouette, A., Design of a Bending Wave Loudspeaker, Department of Applied Acoustics, Chalmers University of Technology 2004

[6] Bonhoff, H., Optimization of vibrating panel loudspeakers, Department of Applied Acoustics, Chalmers University of Technology 2005

[7] Beranek, L., Noise and Vibration Control, Institute of noise control Engineering, Washington DC, 1988.

[8] Harris, N., Hawksford, M.O., The Distributed-Mode Loudspeaker as a Broad-Band Acoustic Radiator, 103rd AES Convention, New York, 1997.

[9] Harris, N., Panzer, J.W., Distributed Mode Loudspeaker Simulation Model, 104th AES Convention, Amsterdam 1998.

[10] Azima, H., Mapp, P., Diffuse Field Distributed-Mode Radiators and their Associated Early Reflections, 104th AES Convention, Amsterdam 1998.

[11] Roberts, M., Exciter design for Distributed Mode Loudspeakers, 104th AES Convention, Amsterdam 1998

[12] Morse, J., Ingard, N., Theoretical acoustics. Mcgraw Hill.

[13] Falk, Patrik., Automatiskt mätsystem för XY-RIGG. Teknisk Akustik Depatment, Chalmers University of Technology 1993

[14] Rife, D,. MLSSA Reference Manual. DRA laboratories. 1987

[15] Keele, D.B., Low frequency Loudspeaker Assesment by nearfield Sound-Pressure Measurement, 94th AES convention, New York 1974.

[16] Brüel & Kjaer, Instructions and applications of the Complex Modulus Apparatus, Copenhagen.

[17] John Borwick, Loudspeakers and Headphones Handbook. Focal Press 2001

[18] Mapp, Peter., Gontcharov,V., Evaluation of Diffuse Mode Loudspeakers in Sound Reinforcement and PA Systems.

[19]Hamada, H., Kirkeby, O., Nelson, P., The "Stereo Dipole" A Virtual Source Imaging System Using Two Closely Spaced Loudspeakers. AES Journal, Volume 46 Number 5. 1998

Websites

[A] http://www.manger-audio.co.uk

[B] http://www.simetric.co.uk/si_materials.htm

[C] http://www.mse.cornell.edu/courses/engri111/modulus.htm

[D] http://www.patentstorm.us/patents/6031926-description.html

[E] http://www.rohacell.com

[F] http://www.si-5.com/

[G] http://www.mlssa.com

[H] http://www.swedac-acoustics.se

Appendix

A. **Equipment list**

B. **Anechoic Measurements results.**

C. **Set-up photos**

D. **MATLAB® routines**

A. Equipment list

Transfer function measurements:

- X-Y system:

  - Control module GS-C200

  - Driving unit control

  - Network card

  - Macintosh plus with X-Y control software

  - Toshiba 5200/100 with MLSSA system

- Yamaha M-35 Power Amplifier.
- Omnidirectional Electret Condenser microphone WM-60A.

  - Sensitivity: -62 ± 3dB

- Sonic Impact Soundpads.

  - Impedance: 8 Ohms

  - Power rating: 6W according to IEC 268-5

  - Weight: 80 grams

Young modulus measurements:

- Brüel&Kjaer Complex Modulus Apparatus type 3930
- Larson & Davis Power Amplifier 2200C
- Yamaha M-35 Power Amplifier.

Mechanical impedance measurement:

- Brüel&Kjaer Force Transducer Type 8203.
- Yamaha M-35 Power Amplifier.
- ENDEVCO Accelerometer Model 25B.
- Brüel&Kjaer Nexus Conditioning Amplifier.
- VXI acquisition station.
- TriggerHappy integrated software.

Piezoelectric Transfer Function measurements:

- Hitachi Oscilloscope V-212.
- High voltage Amplifier LE 150/025.

- X-Y system:
  - Control module GS-C200

  - Driving unit control

  - Network card

  - Macintosh plus with X-Y control software

  - Toshiba 5200/100 with MLSSA system
- Omnidirectional Electret Condenser microphone WM-60A.
  - Sensitivity: -62 ± 3dB
- Piezoelectric Exciter.

B. Material testing complementary results
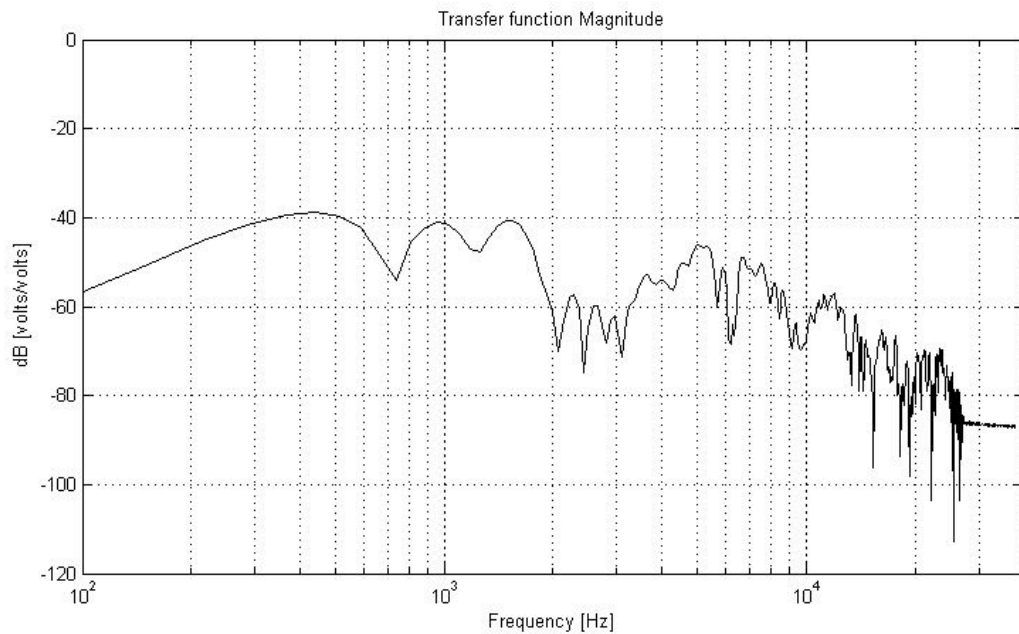
Figure B.1   Anechoic Transfer function magnitude for Polyether foam of h=0.4 cm
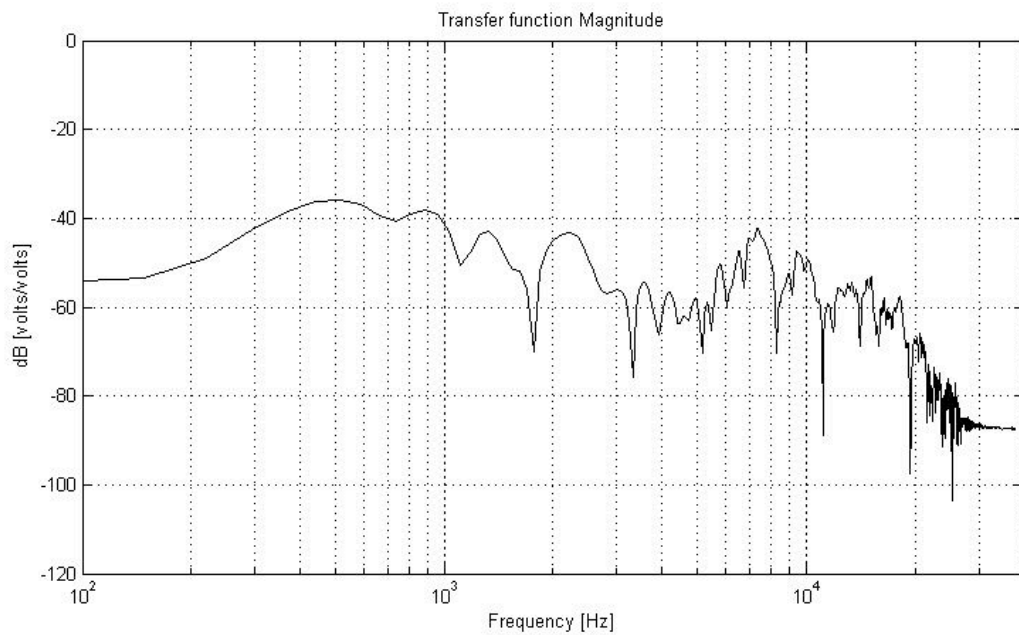
Figure B.2   Anechoic Transfer function magnitude for Polyether foam with and attached interlayer of h=0.3 cm
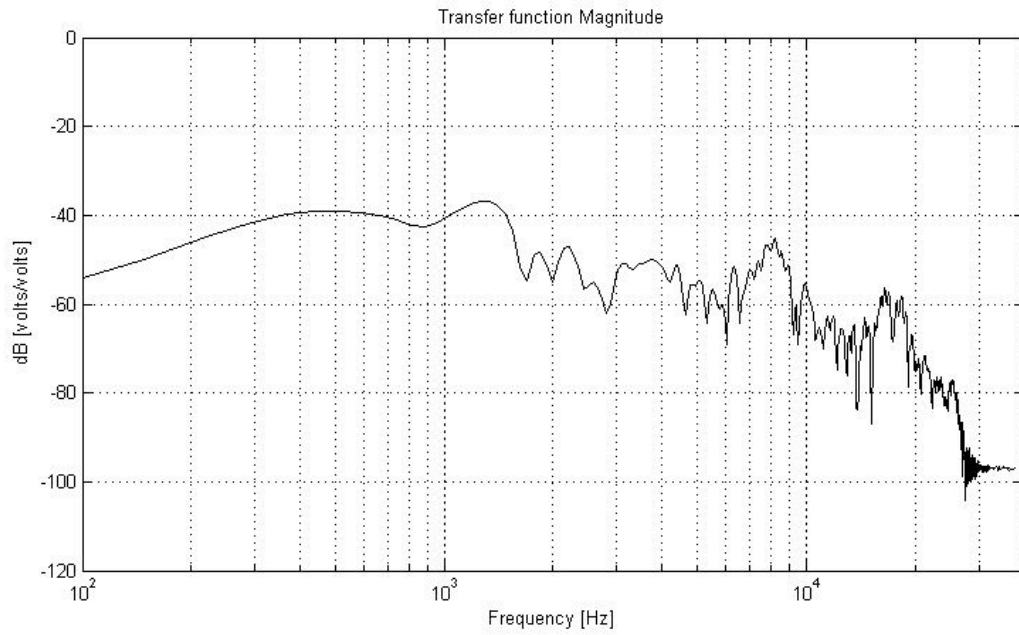
Figure B.3:   *Transfer function magnitude for Polyether foam with and attached interlayer of h=0.5 cm*
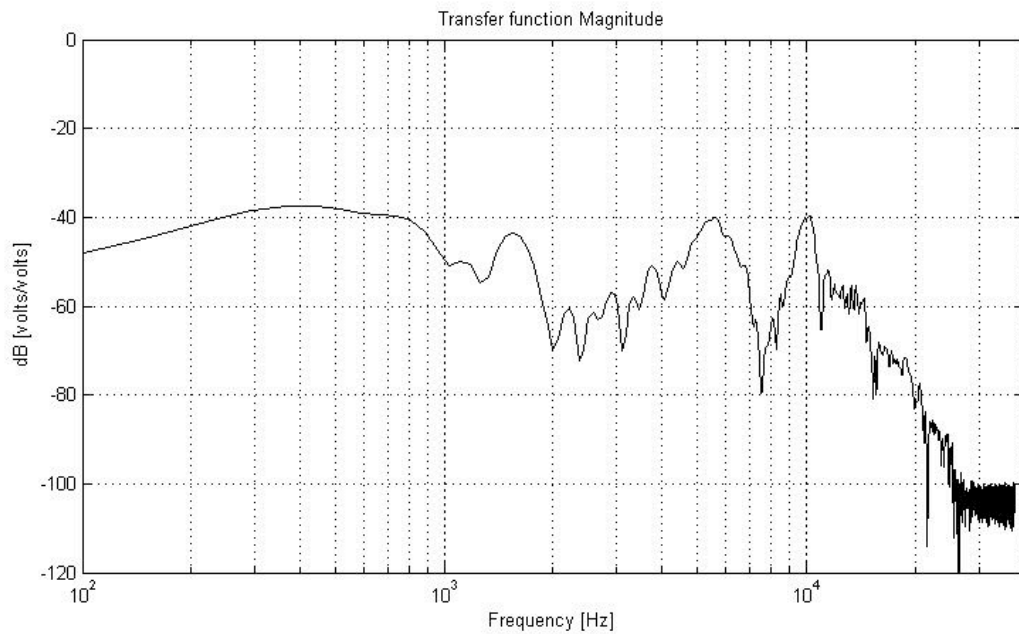
Figure B.4   Anechoic Transfer function magnitude for Polyether foam with and attached interlayer of h=1 cm
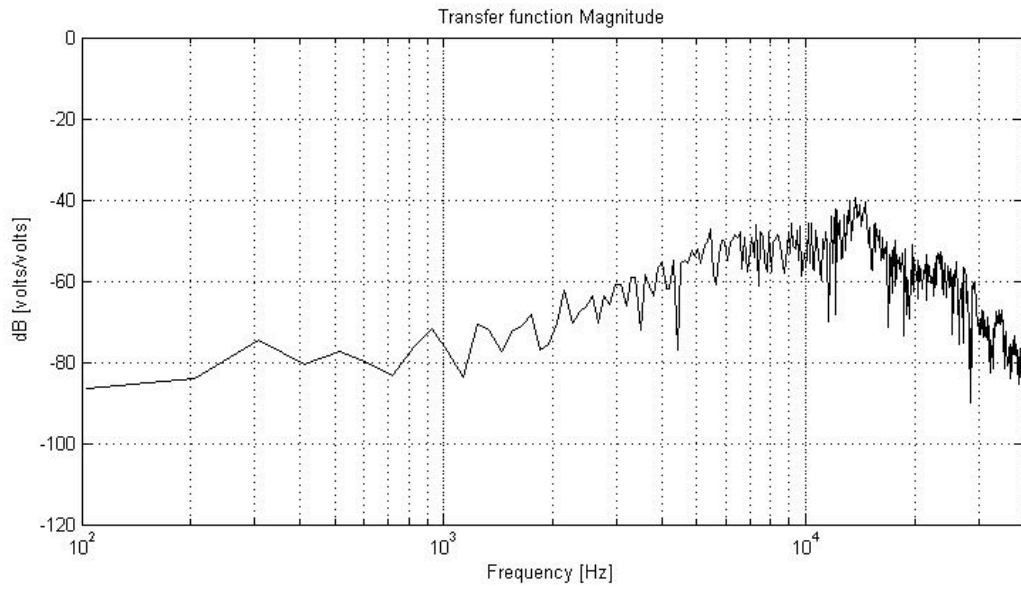
Figure B.5   Transfer Function Magnitude for the brass exciter, panel of 0.3 cm
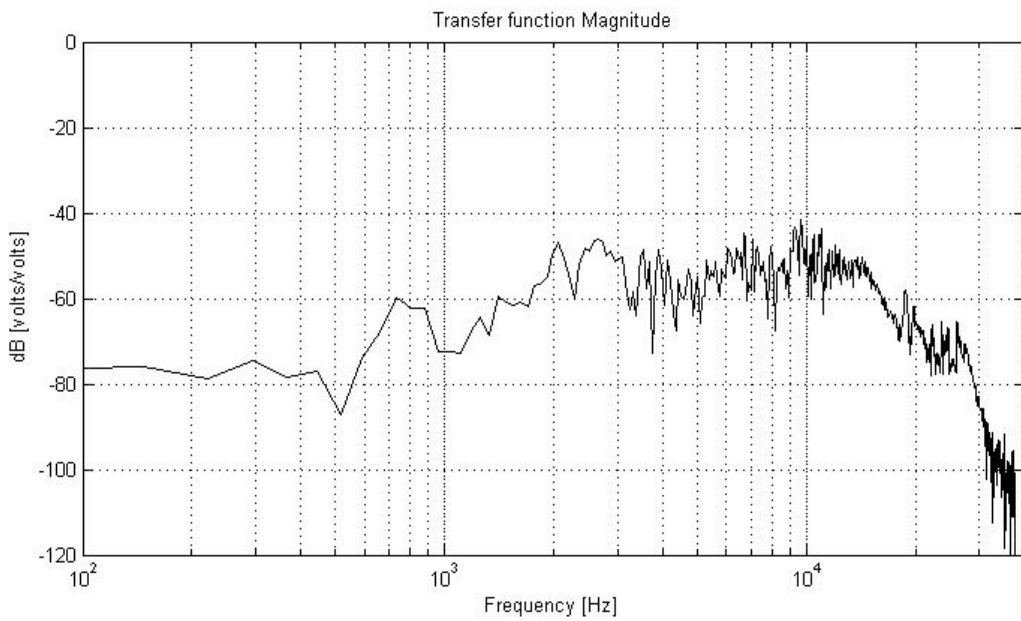
Figure B.6   Transfer Function Magnitude for the brass exciter, panel of 0.4cm
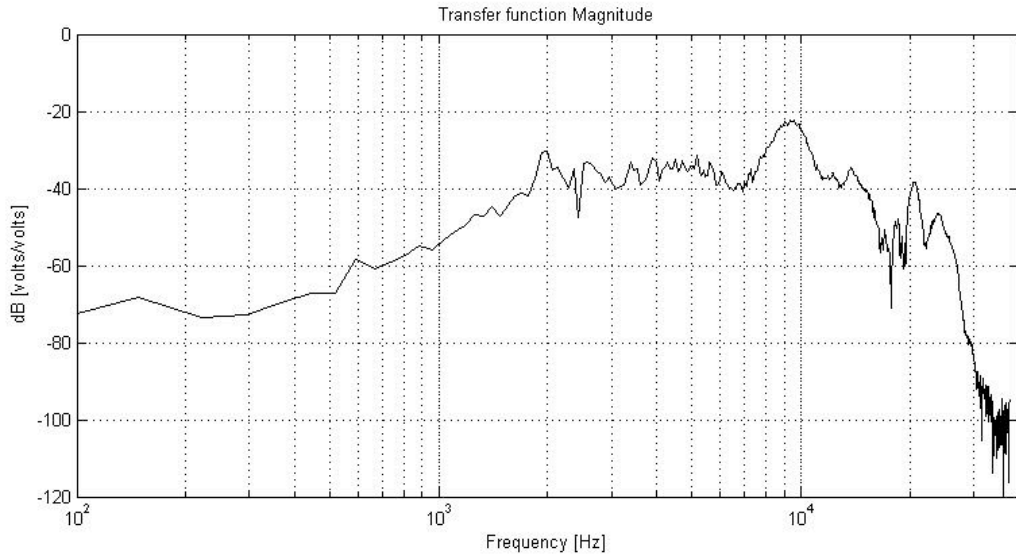
Figure B.7   *Transfer Function Magnitude for the brass exciter, panel of 1 cm*
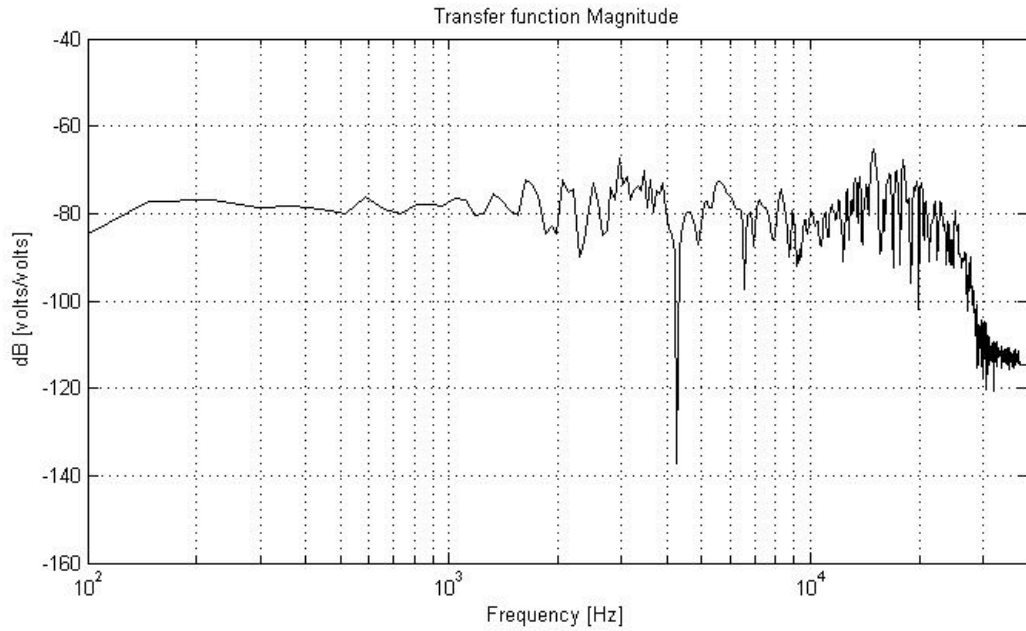
Figure B.8   *Transfer Function Magnitude for the piezoelectric exciter, panel of 0.4 cm.*
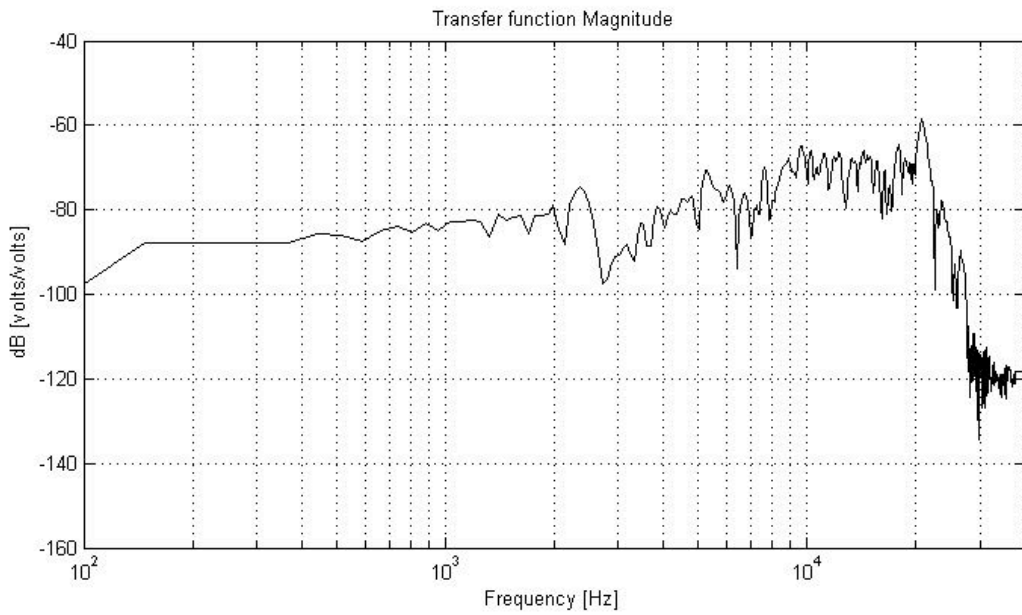
Figure B.9 Transfer Function Magnitude for the piezoelectric exciter, panel of 0.5 cm
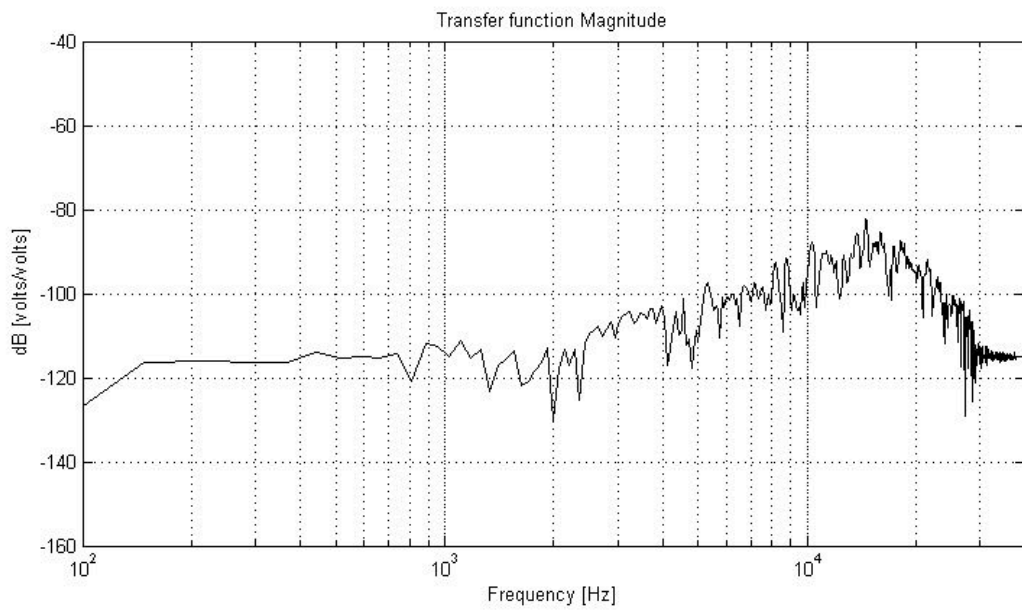
Figure B.10   Transfer Function Magnitude for the piezoelectric exciter, panel of 1 cm

C. Set-up photos

Figure C.1   *Near-field transfer function measurements*

Figure C.2   *Anechoic transfer function measurements*
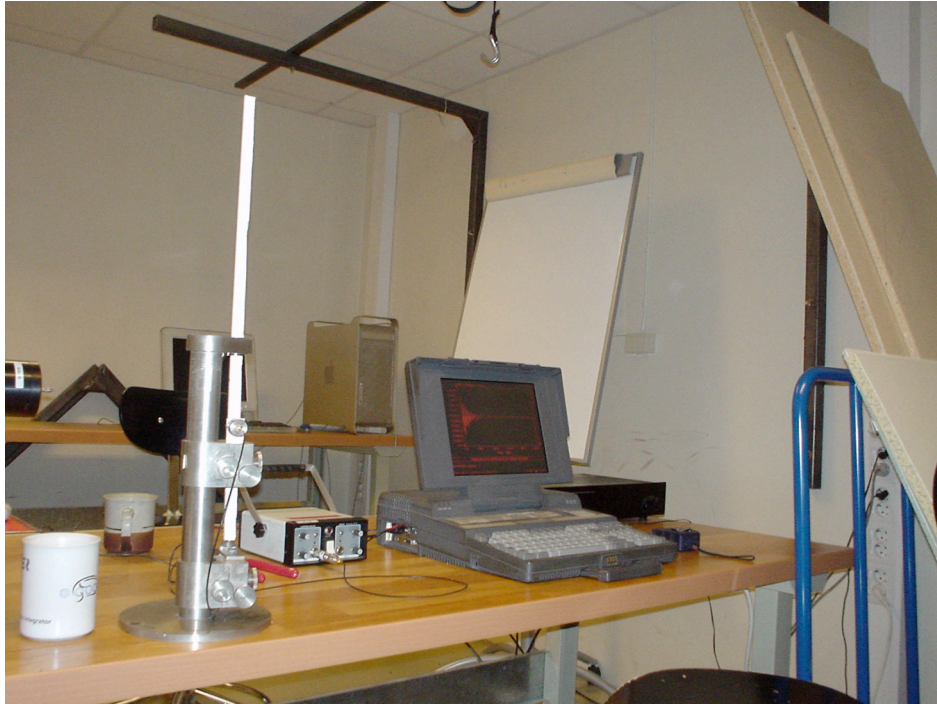
Figure C.3   *Young modulus apparatus measurements*
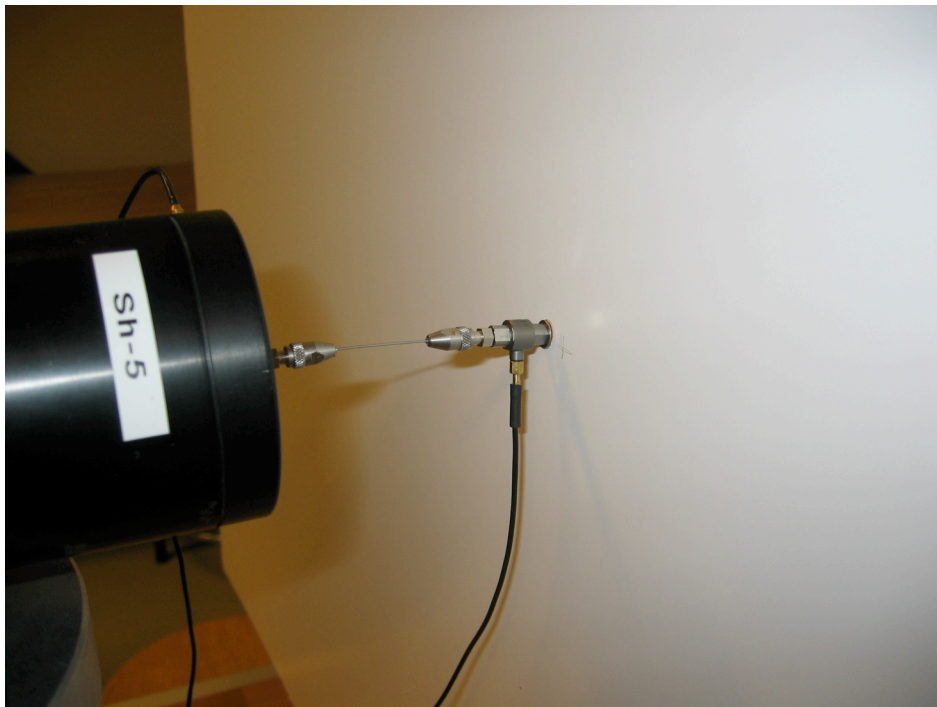
Figure C.4   *Mechanical impedance measurements.*

D. MATLAB® routines

Sound Power level code

```
clear all
clc


rho = 1.21 ;                        % Density of air. [Kg/m^3]
f = 20:10:20000;                    % Frequency vector.
h = 0.003;                          % Thickness plate [m]
mat_density_1 = 163;                % Material density [Kg/m^3]

m = mat_density_1*h;                % Mass per area [kg/m^2]

c_air = 343;                        % Velocity of air. [m/s]
w = 2*pi*f;                         %  [rad]
k = w/c_air;

E_mat = 2.29e8;                     % Modulus of elasticity [N/m^2]
poisson = 0.3;                      % Poisson constant

B = E_mat*h^3/(12*(1-poisson^2)); % Bending Stiffness

k_b = (m/B)^0.25*sqrt(w);

 for i = 2:length(f)

 k_r = 0:k(i)/1000:k(i-1);
 constant = rho*c_air*w(i)^2/(4*pi*B^2);
 integral = k(i)*k_r./((k_r.^4-k_b(i)^4).^2.*sqrt(k(i)^2-k_r.^2));
 Power(i) = constant*trapz(integral);

 end

 W_ref =1e-12;                      % Reference power level.[Watts]
 L_p = 10*log10(Power./W_ref);

 figure(1)
 semilogx(f,L_p,'k')
 grid on
 axis([100 20000 40 150])
 title('Sound power level of a Polyethylene structure of h=0.3')
 xlabel('Frequency [Hz]')
 ylabel('Sound power level [dB re 1e-12 Watts]')
```

Driving point mobility code

```
clear all
clc

rho = 1.21 ;                    % Density of air. [Kg/m^3]
f = 1:2:20000;                  % Frequency vector.
h2 = 0.003;                     % Thickness of the panel [m]
mat_density = 163;             % [Kg/m^3]
m = mat_density*h2;            % Mass per unit area [Kg/m^2]
c_air = 343;                    % Velocity of air. [m/s]
w = 2*pi*f;                     %  [rad]

E_mat = 2.29e8;
poisson = 0.3;
B = E_mat*h2^3/(12*(1-poisson^2));

Z_m = 8*sqrt(B*m);             % Purely resistive panel impedance
bl = 2;

i = 1/8^0.5;

M_mag = 60e-3;
M_coil = 0.25e-3;
R_m = 50;
C_sus = 1.17e-4;
Ree = 7.21;
fre = 71500;
ExpoRe = 1.164;
Le = 62.07e-6;
ExpoLe = 0.875;

Z_par = (Z_m + j*w*M_coil)*M_mag/(Z_m + j*w*M_coil+M_mag);
Z_e = Ree.*(1+f./fre).^ExpoRe +
(j.*w.*Le).^((1+ExpoLe.*(w.*Le./Ree).^2)./(1+(w.*Le./Ree).^2));
Z_tot = Z_par +R_m + 1./(j*w*C_sus);

F = bl*2.83./Z_e;
Y_tot = 1./Z_tot;
v3 = 20*log10(abs(Y_tot.*F));

  figure(3)
  semilogx(f,v3,'k')
  grid on
  title('Driving Point velocity')
  xlabel('Frequency [Hz]')
  ylabel('[dB]')
  axis([1 20000 -65 -30])
```

Critical frequency code

```
[mlsvec,mlsfs,stimulus_amp,mlsdf] = readmls('EV-84.frq','EV-84','Withir')
inc = mlsdf;
f = 0:inc:mlsfs/2;
f1 = 20:10:20000;
db = 20*log10(abs(mlsvec'));

%Finding the resonance frequencies
f_res2 = inc*find(db==max(db));
f_res3 = inc*find(db==max(db(400/inc:700/inc)));
f_res4 = inc*find(db==max(db(1000/inc:1500/inc)));

length1 = 18.3;    % [cm]
density1 = 0.11;   % [gr/cm^3]
h1 = 0.5;          % [cm]
Kn_2 = 22;

E = (48*pi^2*density1*((length1^2/h1)*(f_res2/Kn_2))^2)*1e-1;  %[N/m^2]

h_2 = 0.003                  %[Thickness in meters]
density_2 = 163;             %[Kg/m^3]
m_l = density_2*h_2;         %[Kg/m^2]
poisson = 0.3;               % Poisson constant

B = E*h_2^3/(12*(1-poisson^2));
critical_f = (343^2/(2*pi))*sqrt(m_l/B);

semilogx(f,db,'k')
hold on
grid
axis([0 2000 -80 10])
title('Transfer function Magnitude')
xlabel('Frequency [Hz]')
ylabel('dB [volts/volts]')
```